Ionic liquid characteristics of 1-alkyl-*n*-cyanopyridinium and 1-alkyl-*n*-(trifluoromethyl)pyridinium salts†

Christopher Hardacre,[a] John D. Holbrey,*[a] Claire L. Mullan,[a] Mark Nieuwenhuyzen,[b] W. Matthew Reichert,[c] Kenneth R. Seddon[a] and Simon J. Teat[d]

Received (in Durham, UK) 26th March 2008, Accepted 30th May 2008
First published as an Advance Article on the web 18th July 2008
DOI: 10.1039/b805063e

1-Alkyl-*n*-cyanopyridinium and 1-alkyl-*n*-(trifluoromethyl)pyridinium salts have been synthesised and characterised in order to compare the effects of different electron-withdrawing functional groups on their ability to form ionic liquids. The presence of the electron-withdrawing nitrile or trifluoromethyl substituent on the pyridinium ring leads to salts with higher melting points than with the corresponding 1-alkylpyridinium or 1-alkylpicolinium cations. Solid-state structures were determined by single crystal X-ray crystallography for seven salts; 1-methyl-4-cyanopyridinium methylsulfate, and 1-methyl-3-cyanopyridinium, 1-methyl-4-cyanopyridinium, 1-ethyl-2-cyanopyridinium, 1-ethyl-3-cyanopyridinium, 1-ethyl-4-cyanopyridinium and 1-ethyl-4-(trifluormethyl)pyridinium bis{(trifluoromethyl)sulfonyl}imide, and show the effects of ring-substitution position on hydrogen-bonding in the solid-state and on melting points.

The families of salts that can support the formation of an ionic liquid phase continue to grow, fuelled by the expanding interest in using ionic liquids as solvents for green chemistry, synthesis, electrochemistry, and in materials applications.[1] The physical, chemical and solvent characteristics of ionic liquids (acidity, solvent properties, miscibility, *etc.*) vary considerably with the chemical nature of the ions present, and the behaviour can be further complicated by the potential for competing ion–ion and ion–solute interactions when solutes are added.

Thus, there is a need to develop structure–property relationships for ionic liquids,[2] particularly with respect to group contributions supported by data on new ionic liquid-forming salts. This is of particular interest with respect to designing ionic liquid-forming materials that incorporate specific functional groups, for example in the search for energetic ionic liquids[3,4] or 'task-specific' ionic liquids for metal complexation and extraction.[5]

Partitioning of aromatics between such ionic liquids and alkanes[6,7] suggests that these ionic liquids could be used for aromatic extraction or entrainment. We have previously shown that aromatic molecules, such as benzene, dissolve in ionic liquids to form liquid clathrates, with a strong correlation between the aromatic solutes and the ionic liquid cations,[8] and that the partitioning of dibenzothiophene, a polyaromatic sulfur compound, from hydrocarbons by ionic liquids[9] depends strongly on the structure of the ionic liquid cation. This is most probably as a result of the attractive interactions between aromatics and organic cations.[10] It was envisaged that these attractive interactions could be increased by enhancing the π-acceptor capability of the ionic liquid cation, leading to the development of new extractive desulfurisation technologies.

To this end, we set out to determine the effect that cation modification, by the incorporation of electron-withdrawing groups (EWGs), would have on the propensity of 1-alkylpyridinium salts to form ionic liquids. The functions chosen for this study were nitrile and trifluoromethyl.

Ionic liquids incorporating nitrile groups have been described by Dyson and co-workers;[11,12] however, in these systems, the nitrile group is appended as a terminal functionality onto the alkyl chain of the cation, rather than directly onto the charge-bearing aromatic ring. Even when used as a pendant functional group, Dyson and co-workers[12] have shown that the electron-withdrawing properties of the nitrile group can influence hydrogen/deuterium exchange rates at the C(2)-position of the imidazolium cation. Similarly, ionic liquids containing cations with partially fluorinated alkyl substituents have been described.[13,14] Katritzky and co-workers[3] demonstrated how ionic liquids could be prepared from imidazoles bearing electron-withdrawing nitro- and dicyano-ring substituents, but noted that the presence of the EWGs tended to destabilise the heterocyclic cation relative to the azole, and that the EWGs allowed the formation of ionic liquids containing azolate anions.[4]

1-Alkyl-4-cyanopyridinium iodide salts have been extensively studied in the past with respect to their ability to form ion pair

---

[a] *QUILL Research Centre, The Queen's University of Belfast, Belfast, Northern Ireland, UK BT9 5AG.*
E-mail: j.holbrey@qub.ac.uk; quill@qub.ac.uk
[b] *The Department of Chemistry and Chemical Engineering, The Queen's University of Belfast, Belfast, Northern Ireland, UK BT9 5AG*
[c] *Chemistry Department, Naval Research Academy, Annapolis, MA 21402, USA*
[d] *Advanced Light Source, Lawrence Berkeley National Laboratory, 1 Cyclotron Road, Berkeley, CA 94720, USA*

† Electronic supplementary information (ESI) available: IR spectra of selected systems, and labelled plots of the crystallographic asymmetric units and principle cation–anion hydrogen bonds in the crystal structures of **1**, **2**, **4**, **22**, **24**, **32** (and closest contacts for **37**). CCDC 646907, 646908 and 690235–690239. For crystallographic data in CIF or other electronic format, see DOI: 10.1039/b805063e

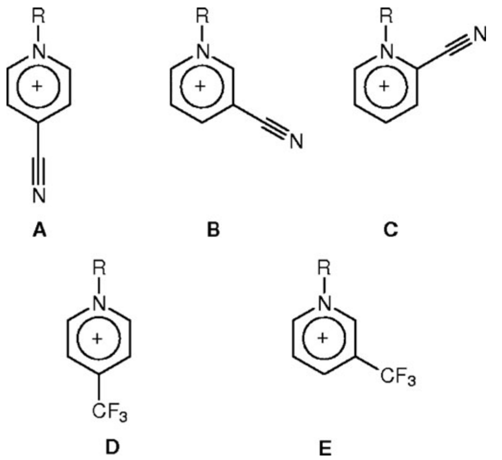

Fig. 1 Cations of the ionic liquids prepared and characterised here: 1-alkyl-4-cyanopyridinium (**A**; R = methyl, ethyl, butyl, hexyl, octyl, dodecyl and hexadecyl; **1–20**), 1-alkyl-3-cyanopyridinium (**B**; R = methyl, ethyl and butyl; **21–28**), 1-alkyl-2-cyanopyridinium (**C**; R = methyl and ethyl; **29–33**), 1-methyl-4-(trifluoromethyl)pyridinium (**D**; **34** and **35**) and 1-methyl-3-(trifluoromethyl)pyridinium (**E**; **36** and **37**). All are denoted as $[\mathrm{C}_n{}^m\mathrm{Xpy}]^+$, where n is length of the alkyl substituent, m is the ring substitution position and X denotes the ring substituent (either CN or $\mathrm{CF_3}$).

charge-transfer complexes in solution,[15] and they have been used as solvatochromatic charge-transfer indicators to study the polarity of solvent systems[16] and as photoinitiators for electron transfer reactions.[17] In addition, the mesomorphic characteristics of several long chain 1-alkyl-4-cyanopyridinium bromide salts (with alkyl substituents longer than dodecyl) have been described,[18] and the related 1-benzyl-2-cyanopyridinium hexafluoroantimonate salt has been used as a catalyst for the photopolymerisation of epoxides.[19]

The 1-alkyl-4-cyanopyridinium halide salts previously reported[20] all have melting points above 100 °C; however, it seemed reasonable that ionic liquids could be prepared by introducing an anion such as bis{(trifluoromethyl)sulfonyl}-imide ($[\mathrm{NTf_2}]^-$).[13]

Here, we describe the synthesis and characterisation (chemical and physical) of new ionic liquids containing 1-alkyl-*n*-cyanopyridinium cations, with related 1-ethyl-*n*-(trifluoromethyl)pyridinium cations (Fig. 1) being prepared for comparison. The single crystal X-ray structures of seven salts; 1-methyl-3-cyanopyridinium, 1-methyl-4-cyanopyridinium, 1-ethyl-2-cyanopyridinium, 1-ethyl-3-cyanopyridinium, 1-ethyl-4-cyanopyridinium and 1-ethyl-4-(trifluoromethyl)pyridinium bis{(trifluoromethyl)sulfonyl}imide, as well as 1-methyl-4-cyanopyridinium methylsulfate, have been determined.

Experimental section

Materials

All chemicals were used as received; cyanopyridines, sodium hexafluorophosphate and the alkylating agents were purchased from Aldrich, and $\mathrm{Li[NTf_2]}$ was purchased from 3 M. The salts were initially prepared by the alkylation of substituted pyridines (4-cyanopyridine, 3-cyanopyridine, 2-cyanopyridine, 4-(trifluoromethyl)pyridine and 3-(trifluoromethyl)pyridine) with dimethylsulfate, diethylsulfate or alkylbromides, followed by metathesis in water with $\mathrm{Li[NTf_2]}$ or sodium hexafluorophosphate.

1-Methyl-4-cyanopyridinium methylsulfate (1)

A solution of 4-cyanopyridine (30 g, 0.3 mol) and dimethylsulfate (40 $\mathrm{cm^3}$) in ethanenitrile (100 $\mathrm{cm^3}$) was heated with stirring to 45 °C for 24 h. On cooling to room temperature, the product precipitated as colourless crystals, mp 108–115 °C (Found: C, 38.07; H, 3.92; N, 11.34. $\mathrm{[C_7H_7N_2][CH_3SO_4]}$ requires C, 41.73; H, 4.38; N, 12.17%); δ_H (500 MHz, DMSO-d_6) 9.28 (2H, d, J = 6.45 Hz), 8.68 (2H, d, J = 6.45 Hz), 4.44 (3H, s), 3.38 (2H, s).

1-Methyl-4-cyanopyridinium bis{(trifluoromethyl)sulfonyl}imide (2)

The metathesis of **1** (50 g, 0.22 mol) in water with $\mathrm{Li[NTf_2]}$ (62 g, 1 equiv.) resulted in separation of the ionic liquid as a colourless liquid, which was collected and washed with water. On standing, the ionic liquid spontaneously crystallised, and was collected by filtration and dried in air as a colourless crystalline solid, mp 65–66 °C (Found: C, 26.75; H, 1.70; N, 10.32. $\mathrm{[C_7H_7N_2][NS_2O_4C_2F_6]}$ requires C, 27.07; H, 1.77; N, 10.85%); δ_H (500 MHz, DMSO-d_6) 9.28 (2H, d) 8.68 (2H, d), 4.43 (3H, s).

1-Ethyl-4-cyanopyridinium ethylsulfate (3)

A solution of 4-cyanopyridine (10.4 g, 0.1 mol) and diethylsulfate (15.4 g, 0.1 mol) in toluene (75 $\mathrm{cm^3}$) was heated with stirring at reflux for 6 h, resulting in the formation of a biphasic system. The lower dense pale yellow liquid phase was separated from the reaction mixture, washed with toluene (20 $\mathrm{cm^3}$) and hexane (2 × 30 $\mathrm{cm^3}$), dried under reduced pressure with heating at 70 °C and then *in vacuo* to give the ethylsulfate salt (yield 80%) as a pale yellow viscous liquid, T_g = −71 °C (Found: C, 45.36; H, 5.02; N, 10.75. $\mathrm{[C_8H_9N_2][C_2H_5SO_4]}$ requires C, 46.50; H, 5.46; N, 10.85%); δ_H (500 MHz, DMSO-d_6) 9.38 (2H, d), 9.37 (2H, d), 4.71 (2H, q), 3.73 (2H, q), 1.55 (3H, t), 1.09 (3H, t).

1-Ethyl-4-cyanopyridinium bis{(trifluoromethyl)sulfonyl}imide (4)

The metathesis of a solution of **3** (8.00 g, 0.03 mol) in water (25 $\mathrm{cm^3}$) with aqueous $\mathrm{Li[NTf_2]}$ (8.83 g, 1 equiv. in 25 $\mathrm{cm^3}$ $\mathrm{H_2O}$) resulted in separation of the ionic liquid as a cloudy liquid phase. The mixture cleared to two transparent liquid phases on heating to 70 °C, and the lower yellow ionic liquid was collected, washed with water, dried under reduced pressure and finally *in vacuo* with heating at 80 °C to yield a clear colourless liquid immiscible with dichloromethane, which reversibly changes colour on contact with water to intense yellow. The colourless ionic liquid crystallised on standing at room temperature as a colourless crystalline solid (89% yield), mp 33–35 °C (Found: C, 29.22; H, 1.79; N, 10.25. $\mathrm{[C_8H_9N_2][NS_2O_4C_2F_6]}$ requires C, 29.06; H, 2.19; N, 10.17%); δ_H (500 MHz, DMSO-d_6) 9.37 (2H, d), 8.68 (2H, d), 4.70 (2H, q), 1.56 (3H, t); δ_H (500 MHz, $\mathrm{CD_3CN}$) 8.93 (2H, d), 8.38 (2H, d), 4.68 (2H, q), 1.64 (3H, t); δ_C (125 MHz,

CD_3CN) 145.44, 131.02, 127.89, 123.39, 120.84, 118.29, 117.11, 115.74, 113.72, 58.36, 15.08, 0.04.

1-Ethyl-4-cyanopyridinium hexafluorophosphate (5)

To a stirred solution of **3** (5.62 g, 0.0218 mol) in water (10 cm^3) was added a solution of sodium hexafluorophosphate (3.66 g, 1 equiv.) in water (15 cm^3). A colourless precipitate formed immediately and was collected by filtration, washed with water, and air dried to give the product as a microcrystalline powder (yield 4.65 g, 55%), mp 176 °C (Found: C, 34.03; H, 3.60; N, 9.92. $[C_8H_9N_2][PF_6]$ requires C, 34.55; H, 3.26; N, 10.07%); δ_H (500 MHz, DMSO-d_6) 9.35 (2H, d), 8.69 (2H, d), 4.68 (2H, q), 1.55 (3H, t).

1-Butyl-4-cyanopyridinium bromide (6)

4-Cyanopyridine (20.8 g, 0.2 mol) and bromobutane (42 g, 1.5 equiv.) were combined and heated with stirring at 135 °C in a round-bottomed flask sealed with a Safe-Lab® pressure seal. After heating for 18 h, the resultant yellow solid mass was filtered rapidly to remove excess bromobutane, washed with ethyl acetate, which removed the yellow colouration, and then dried under reduced pressure to yield a pale cream-coloured microcrystalline powder (yield 76%), mp 212 °C (Found: C, 49.89; H, 5.38; N, 11.63. $[C_{10}H_{13}N_2]Br$ requires C, 49.81; H, 5.43; N, 11.62%); δ_H (500 MHz, DMSO-d_6) 9.44 (2H, d), 8.71 (2H, d), 4.47 (2H, t), 1.90 (2H, m), 1.29 (2H, m), 0.89 (3H, t).

1-Butyl-4-cyanopyridinium bis{(trifluoromethyl)sulfonyl}imide (7)

7 was prepared from **6** and Li[NTf_2] by the same procedure used for **4**. The lower ionic liquid phase was separated, extracted into dichloromethane, and dried with heating under reduced pressure to give a clear, pale yellow liquid (yield 78%) that was immiscible with water or $CHCl_3$ and soluble in DMSO. T_g = −64 °C (Found: C, 31.86; H, 2.74; N, 9.46. $[C_{10}H_{13}N_2][NS_2O_4C_2F_6]$ requires C, 32.66; H, 2.97; N, 9.52%); δ_H (500 MHz, DMSO-d_6) 9.35 (2H, d), 8.69 (2H, d), 4.65 (2H, t), 1.90 (3H, tt), 1.292 (2H, tt), 0.90 (3H, t).

1-Butyl-4-cyanopyridinium hexafluorophosphate (8)

8 was prepared by the anion metathesis of **6** in water with a sodium hexafluorophosphate solution. The product precipitated and was collected by filtration, dried in air, and then heated at 50 °C *in vacuo* to give a colourless microcrystalline powder (yield 73%), mp 140 °C (Found: C, 38.80; H, 4.29; N, 9.18. $[C_{10}H_{13}N_2][PF_6]$ requires C, 39.23; H, 4.28; N, 9.15%); δ_H (500 MHz, DMSO-d_6) 9.32 (2H, d), 8.66 (2H, d), 4.65 (2H, t), 1.90 (2H, tt), 1.30 (2H, tt), 0.90 (3H, t).

1-Hexyl-4-cyanopyridinium bromide (9)

9 was prepared from 4-cyanopyridine (104 g, 1 mol) and bromohexane (200 cm^3, 1.6 mol) in toluene (300 cm^3) in a pressure vessel heated to 160 °C for 24 h. On cooling to room temperature, the product precipitated as a colourless crystalline solid, which was collected by filtration, washed with ether and then dried under vacuum (100 g, ~50% yield), mp 195–197 °C (Found: C, 53.45; H, 5.99; N, 10.53. $[C_{12}H_{17}N_2]Br$ requires C, 53.54; H, 6.37; N, 10.41%); δ_H (500 MHz, DMSO-d_6) 9.82 (2H, d), 9.11 (2H, d), 4.65 (2H, t), 2.30 (2H, m), 1.30 (6H, tt), 0.90 (3H, t).

1-Hexyl-4-cyanopyridinium bis{(trifluoromethyl)sulfonyl}imide (10)

10 was prepared from **9** and Li[NTf_2] using the procedure described for **4**. The dense yellow liquid was collected, extracted into dichloromethane, dried over anhydrous Na_2SO_4 and the solvent removed *in vacuo* to give a pale yellow liquid (T_g = −59 °C), which crystallised upon storage in a freezer as a colourless solid, mp 10 °C (Found: C, 35.86; H, 3.52; N, 8.96. $[C_{12}H_{17}N_2][NS_2O_4C_2F_6]$ requires C, 35.82; H, 3.65; N, 8.95%); δ_H (500 MHz, DMSO-d_6) 9.88 (2H, d), 9.11 (2H, d), 5.09 (2H, t), 2.27 (2H, m), 1.62 (6H, m) 1.19 (3H, t).

1-Hexyl-4-cyanopyridinium hexafluorophosphate (11)

11 was prepared by the anion metathesis of **9** in water with a sodium hexafluorophosphate solution. The product precipitated and was collected by filtration, dried in air, and then heated at 50 °C *in vacuo* to give a colourless microcrystalline powder, mp 115 °C (Found: C, 43.12; H, 5.13; N, 8.28. $[C_{12}H_{17}N_2][PF_6]$ requires C, 41.57; H, 4.64; N, 8.07%); δ_H (500 MHz, DMSO-d_6) 9.69 (2H, d), 9.04 (2H, d), 5.00 (2H, t), 2.26 (2H, m), 1.61 (6H, m), 1.19 (3H, t).

1-Octyl-4-cyanopyridinium bromide (12)

12 was prepared from 4-cyanopyridine (104 g 1.0 mol) and bromooctane (200 cm^3, 1.6 mol) in toluene (300 cm^3) in a pressure vessel heated to 160 °C for 24 h. After cooling to room temperature, the product precipitated upon addition of ethyl acetate as a colourless hygroscopic microcrystalline powder, which was collected by filtration and dried under vacuum (100 g, ~50% yield), mp 162 °C (Found: C, 58.00; H, 7.09; N, 9.18. $[C_{14}H_{21}N_2]Br$ requires C, 56.57; H, 7.12; N, 9.42%); δ_H (500 MHz, $CDCl_3$) 9.90 (2H, d), 8.50 (2H, d), 5.05 (2H, t), 4.05 (2H, q), 2.04 (2H, m), 1.31 (2H, m), 1.30 (2H, m), 1.2 (4H, m), 0.80 (3H, t).

1-Octyl-4-cyanopyridinium bis{(trifluoromethyl)sulfonyl}imide (13)

13 was prepared from **12** and Li[NTf_2] using the procedure described for **4**. The dense pale brown liquid was collected, extracted into dichloromethane, dried over anhydrous Na_2SO_4 and the solvent removed *in vacuo* to give a pale yellow liquid that slowly crystallised as colourless plates upon standing, mp 30 °C (Found: C, 39.15; H, 4.46; N, 8.80. $[C_{14}H_{21}N_2][NS_2O_4C_2F_6]$ requires C, 38.63; H, 4.25; N, 8.45%); δ_H (500 MHz, DMSO-d_6) 9.35 (2H, d), 8.69 (2H, d), 4.64 (2H, t), 1.92 (2H, m), 1.25 (10H, m), 0.84 (3H, t).

1-Octyl-4-cyanopyridinium hexafluorophosphate (14)

14 was prepared by the anion metathesis of **12** in water with a sodium hexafluorophosphate solution. The product precipitated as a fine colourless crystalline powder, which was collected by filtration, dried in air and then heated at 50 °C *in vacuo*, mp 122–124 °C (Found: C, 42.56; H, 4.48; N, 7.15. $[C_{14}H_{21}N_2][PF_6]$ requires C, 46.41; H, 5.84; N, 7.73%); δ_H

(500 MHz, DMSO-d_6) 9.30 (2H, d), 8.64 (2H, d), 4.62 (2H, t), 3.47 (s, H_2O), 1.90 (2H, m), 1.25 (10H, m), 0.83 (3H, t).

1-Dodecyl-4-cyanopyridinium bromide (15)

15 was prepared from 4-cyanopyridine (20.82 g, 0.20 mol) and 1-bromododecane (54.83 g, 0.22 mol) in toluene (100 cm^3) in a round-bottomed flask sealed with a Safe-Lab® pressure seal and heated with stirring at 135 °C. After heating for 6 h, the product was filtered rapidly to remove excess 1-bromododecane, washed with ethyl acetate and then dried under reduced pressure to yield a yellow powder (81% yield), mp 196 °C (Found: C, 60.52; H, 7.11; N, 7.96. $[C_{18}H_{29}N_2]Br$ requires C, 61.19; H, 8.27; N, 7.93%); δ_H (500 MHz, DMSO-d_6) 9.420 (2H, d), 8.704 (2H, d), 4.670 (2H, m), 1.915 (2H, m), 1.25 (18H, m), 0.835 (3H, t)

1-Dodecyl-4-cyanopyridinium bis{(trifluoromethyl)sulfonyl}imide (16)

16 was prepared from **15** and Li[NTf_2] using the procedure described for **4** as a fine colourless crystalline powder, which was collected by filtration, dried in air and then *in vacuo*, mp 52 °C, (Found: C, 43.52; H, 5.09; N, 7.71. $[C_{18}H_{29}N_2][NS_2O_4C_2F_6]$ requires C, 43.39; H, 5.28; N, 7.59%); δ_H (500 MHz, DMSO-d_6) 9.342 (2H, d), 8.79 (2H, d), 4.634 (2H, t), 1.909 (2H, m), 1.221 (18H, m), 0.834 (3, t)

1-Dodecyl-4-cyanopyridinium hexafluorophosphate (17)

17 was prepared by the anion metathesis of a heated solution of **15** (1.08 g, 0.0034 mol) in water (20 cm^3) with sodium hexafluorophosphate solution (0.58 g, 0.0034 mol) in water (1 cm^3). The product separated from the hot aqueous solution as a colourless microcrystalline powder, which was collected by filtration and air-dried, mp 146 °C (Found: C, 51.33; H, 6.97; N, 6.70. $[C_{18}H_{29}N_2][PF_6]$ requires C, 51.67; H, 6.99; N, 6.70%); δ_H (500 MHz, DMSO-d_6) 9.37 (2H, d, J = 6.6 Hz), 8.72 (2H, d, J = 6.6 Hz), 4.66 (2H, t, J = 7.42 Hz), 1.94 (2H, m, J = 6.6 Hz), 1.23–1.32 (18H, m), 0.87 (3H, t, J = 6.6 Hz).

1-Hexadecyl-4-cyanopyridinium bromide (18)

18 was prepared from 4-cyanopyridine (20.82 g, 0.20 mol) and 1-bromohexadecane (67.18 g, 0.22 mol) in toluene (100 cm^3) in a round-bottomed flask sealed with a Safe-Lab® pressure seal and heated with stirring at 135 °C. After heating for 6 h, the product was filtered rapidly to remove excess 1-bromohexadecane, washed with ethyl acetate and then dried under reduced pressure to yield a yellow powder (80% yield), mp 196 °C (Found: C, 63.49; H, 8.75; N, 7.92. $[C_{22}H_{37}N_2]Br$ requires C, 64.54; H, 9.11; N, 6.84%); δ_H (500 MHz, DMSO-d_6) 9.385 (2H, d, J = 7 Hz), 8.707 (2H, d, J = 7 Hz), 4.657 (2H, t), 1.907 (2H, m), 1.237 (26H, m), 0.836 (3H, t).

1-Hexadecyl-4-cyanopyridinium bis{(trifluoromethyl)sulfonyl}imide (19)

19 was prepared from a hot solution of **18** (1.25 g, 0.00315 mol) in water (20 cm^3) and a solution of Li[NTf_2] (0.9 g, 0.0032 mol) in water (1 cm^3) using the procedure described for **4**. The product separated from the hot aqueous solution as a viscous oil, which crystallised upon cooling as a yellow solid, mp 68 °C (Found: C, 48.06; H, 6.47; N, 6.34. $[C_{22}H_{37}N_2][NS_2O_4C_2F_6]$ requires C, 47.28; H, 6.12; N, 6.89%); δ_H (500 MHz, DMSO-d_6) 9.40 (2H, d, J = 7.1 Hz), 8.73 (2H, d, J = 7.1 Hz), 4.67 (2H, t, J = 7.56 Hz), 1.92 (2H, m), 1.25 (26 H, m), 0.86 (3H, t, J = 7.2 Hz).

1-Hexadecyl-4-cyanopyridinium hexafluorophosphate (20)

20 was prepared by the anion metathesis of a heated solution of **18** (1.16 g, 0.0029 mol) in water (20 cm^3) with sodium hexafluorophosphate solution (0.5 g, 0.003 mol) in water (1 cm^3). The product separated from the hot aqueous solution as a pale yellow powder, which was collected by filtration and air-dried, mp 180 °C (Found: C, 55.87; H, 8.17; N, 5.34. $[C_{22}H_{37}N_2][PF_6]$ requires C, 55.69; H, 7.86; N, 5.90%); δ_H (500 MHz, DMSO-d_6) 9.57 (2H, d, J = 6.7 Hz), 8.72 (2H, d, J = 6.7 Hz), 4.66 (2H, t, J = 7.51 Hz), 1.93 (2H, m), 1.20–1.32 (26 H, m), 0.87 (3H, t, J = 7.0 Hz).

1-Methyl-3-cyanopyridinium methylsulfate (21)

21 was prepared using the same procedure as **1** from 3-cyanopyridine (30 g, 0.3 mol) and dimethylsulfate (40 cm^3) in ethanenitrile (50 cm^3) as a pale brown liquid, T_g = −68 °C (Found: C, 34.63; H, 4.05; N, 8.86. $[C_7H_7N_2][CH_3SO_4]$ requires C, 41.73; H, 4.38; N, 12.17%); δ_H (500 MHz, DMSO-d_6) 9.66 (1H, s), 9.23 (1H, d, J = 5.9 Hz), 9.05 (1H, d, J = 8.0 Hz), 8.30 (1H, dd, J_1 = 8.0 Hz, J_2 = 5.9 Hz), 4.41 (3H, s), 3.39 (3H, s).

1-Methyl-3-cyanopyridinium bis{(trifluoromethyl)sulfonyl}imide (22)

The metathesis of **21** (40.0 g, 0.166 mol) in water (100 cm^3) with Li[NTf_2] (47.7 g, 1 equiv.) resulted in separation of the ionic liquid as a colourless liquid, which was collected, washed with water and dried *in vacuo* as a colourless crystalline solid, mp 63–65 °C (Found: C, 26.74; H, 1.77; N, 10.45. $[C_7H_7N_2][NS_2O_4C_2F_6]$ requires C, 27.07; H, 1.77; N, 10.52%); δ_H (500 MHz, DMSO-d_6) 9.73 (1H, s), 9.24 (1H, d), 9.06 (1H, d), 8.33 (1H, dd), 4.38 (3H, s).

1-Ethyl-3-cyanopyridinium ethylsulfate (23)

Diethylsulfate (154 g, 1 mol) was added dropwise to a solution of 3-cyanopyridine (104 g, 1 mol) in toluene (250 cm^3) that was heated to 100 °C with stirring. After addition, the reaction mixture was heated for a further 4 h and then cooled to room temperature. The product formed as a dense pale yellow liquid, which was separated, washed with toluene and then with hexane, dried under reduced pressure and finally *in vacuo* to yield a pale yellow viscous liquid (84% yield), T_g = −71 °C (Found: C, 44.00; H, 5.25; N, 10.28. $[C_8H_9N_2][C_2H_5SO_4]$ requires C, 46.50; H, 5.46; N, 10.85%); δ_H (500 MHz, DMSO-d_6) 9.774 (1H, s, C(2)–H), 9.330 (1H, d, C(6)–H), 9.066 (1H, d, C(4)–H), 8.335 (1H, dd, C(5)–H), 4.659 (2H, q), 3.728 (2H, q), 1.556 (3H, t), 1.087 (3H, t); δ_H (500 MHz, MeCN-d_3) 9.49 (1H, s), 9.21 (1H, d), 8.86 (1H, d), 8.26 (1H, dd), 4.77 (2H, q), 3.90 (2H, q), 1.65 (3H, t), 1.20 (3H, t).

1-Ethyl-3-cyanopyridinium bis{(trifluoromethyl)sulfonyl}imide (24)

24 was prepared from **23** (90 g) in water (200 cm^3) with Li[NTf$_2$] (110 g) in water (100 cm^3). The product formed as a colourless crystalline precipitate, which was collected by filtration, washed with water and dried under reduced pressure (89% yield), mp 73 °C (Found: C, 28.91; H, 1.90; N, 10.19. [C$_{10}$H$_{13}$N$_2$][NS$_2$O$_4$C$_2$F$_6$] requires C, 29.06; H, 2.19; N, 10.17%); δ_H (500 MHz, DMSO-*d*$_6$) 9.78 (1H, s, C(2)–H), 9.32 (1H, d, C(6)–H, J = 6.12 Hz), 9.06 (1H, d, C(4)–H, J = 8.12 Hz), 8.33 (1H, dd, C(5)–H, J = 7.9, 6.4 Hz), 4.65 (2H, q, J = 7.324 Hz), 3.43 (2H, q, J = 7.2 Hz), 1.56 (3H, t, J = 7.33 Hz); δ_H (500 MHz, MeCN-*d*$_3$) 9.19 (1H, s), 8.95 (1H, d), 8.82 (1H, d), 8.22 (1H, dd), 4.66 (2H, q), 1.65 (3H, t); δ_C (125.7 MHz, MeCN-*d*$_3$) 148.40, 147.60, 128.83, 123.39, 120.84, 118.30, 117.10, 115.75, 113.88, 112.65, 58.26, 14.85, 0.04.

1-Ethyl-3-cyanopyridinium hexafluorophosphate (25)

25 was prepared by the anion metathesis of **23** (4.5 g) in water (15 cm^3) with a solution of sodium hexafluorophosphate (3.5 g) in water (10 cm^3) as a colourless crystalline precipitate, which was collected by filtration, dried in air and then *in vacuo*, mp 164–167 °C (Found: C, 25.74; H, 2.36; N, 7.38. [C$_{10}$H$_{13}$N$_2$][PF$_6$] requires C, 39.23; H, 4.28; N, 9.15%); δ_H (500 MHz, DMSO-*d*$_6$) 9.78 (1H, s, C(2)–H), 9.32 (1H, d, C(6)–H, J = 6.12 Hz), 9.06 (1H, d, C(4)–H, J = 8.12 Hz), 8.33 (1H, dd, C(5)–H, J = 7.9, 6.4 Hz), 4.65 (2H, q, J = 7.324 Hz), 3.43 (2H, q, J = 7.2 Hz), 1.56 (3H, t, J = 7.33 Hz).

1-Butyl-3-cyanopyridinium bromide (26)

26 was prepared from 3-cyanopyridine (20 g, 0.2 mol) and 1-bromobutane (50 cm^3, excess) in a sealed pressure flask and stirred with heating at 135 °C for 3 h to form a solid yellow mass. After cooling, the product was collected by filtration and washed with ethyl acetate to give a cream powdery solid, mp 155–157 °C (Found: C, 49.94; H, 5.48; N, 12.90. [C$_{10}$H$_{13}$N$_2$]Br requires C, 49.81; H, 5.43; N, 11.62%); δ_H (500 MHz, DMSO-*d*$_6$) 9.897 (1H, d, J = 8.6 Hz), 9.437 (1H, s), 9.094 (1H, dd, J = 1.1, 7.7 Hz), 8.369 (1H, dd, J = 7.7 Hz), 4.67 (2H, dt, J = 7, 6.3 Hz), 3.357 (2H, m, J = 6.62 Hz), 1.926 (2H, m, J = 7.5 Hz), 1.295 (2H, m, J = 7.5 Hz), 0.895 (3H, t, J = 7.4 Hz)

1-Butyl-3-cyanopyridinium bis{(trifluoromethyl)sulfonyl}imide (27)

27 was prepared from **26** (16.82 g) and Li[NTf$_2$] (19.0 g) using the same procedure used for **4**. The resultant cloudy mixture was heated to 60 °C, forming two separate phases. The upper aqueous phase was decanted and the dense product phase was collected, washed with water and dried under vacuum to yield the product as a clear pale brown liquid (yield 78%) (Found: C, 32.37; H, 3.18; N, 9.04. [C$_{10}$H$_{13}$N$_2$][NS$_2$O$_4$C$_2$F$_6$] requires C, 32.66; H, 2.97; N, 9.52%); δ_H (500 MHz, DMSO-*d*$_6$) 9.786 (1H, s, C(2)–H), 9.315 (1H, d, C(6)–H, J = 6.06 Hz), 9.068 (1H, d, C(4)–H, J = 8.13 Hz), 8.335 (1H, dd, C(3)–H, J_1 = 6.06 Hz, J_2 = 8.13 Hz), 4.609 (2H, t, J = 7.5 Hz), 1.925 (2H, m), 1.305 (2H, m), 0.910 (3H, t, J = 7.35 Hz).

1-Butyl-3-cyanopyridinium hexafluorophosphate (28)

28 was prepared by anion metathesis of **26** (0.9 g) in water (10 cm^3) with a solution of sodium hexafluorophosphate (0.7 g) in water (5 cm^3). The product precipitated from the solution as colourless crystals, which were collected by filtration, dried in air and then *in vacuo*, mp 110–111 °C (Found: C, 38.80; H, 4.29; N, 9.18. [C$_{10}$H$_{13}$N$_2$][PF$_6$] requires C, 39.23; H, 4.28; N, 9.15%); δ_H (500 MHz, DMSO-*d*$_6$) 9.81 (1H, s), 9.34 (1H, d, J = 6.26 Hz), 9.10 (1H, d, J = 8.26Hz), 8.37 (1H, dd, J_1 = 6.26 Hz, J_2 = 8.26 Hz), 4.63 (2H, t, J = 7.17 Hz), 1.95 (2H, tt), 1.33 (2H, tt), 0.94 (3H, t, J = 7.6 Hz).

1-Methyl-2-cyanopyridinium methylsulfate (29)

29 was prepared using the same procedure as **1** from 2-cyanopyridine (30 g, 0.3 mol) and dimethylsulfate (40 cm^3) in ethanenitrile (50 cm^3) as a crystalline solid upon removal of solvents *in vacuo*, mp 91 °C (Found: C, 34.54; H, 4.97; N, 9.69. [C$_7$H$_7$N$_2$][CH$_3$SO$_4$] requires C, 41.73 H, 4.38; N, 12.17%); δ_H (500 MHz, DMSO-*d*$_6$) 9.38 (1H, d), 8.90 (1H, d), 8.81 (1H, dd), 4.71 (3H, s).

1-Methyl-2-cyanopyridinium bis{(trifluoromethyl)sulfonyl}imide (30)

The metathesis of **29** (40.0 g, 0.166 mol) in water (100 cm^3) with Li[NTf$_2$] (47.7 g, 1 equiv.) resulted in separation of the ionic liquid as a colourless liquid, which was collected, washed with water and dried *in vacuo* to yield the product as a colourless oil, which slowly solidified upon standing as a colourless crystalline mass, mp 19 °C (Found: C, 26.46; H, 2.34; N, 10.19. [C$_7$H$_7$N$_2$][NS$_2$O$_4$C$_2$F$_6$] requires C, 27.07; H, 1.77; N, 10.52%); δ_H (500 MHz, DMSO-*d*$_6$) 9.39 (1H, d), 8.84 (1H, dd), 8.81 (1H, dd), 8.46 (1H, d), 4.54 (3H, s).

1-Ethyl-2-cyanopyridinium ethylsulfate (31)

Diethylsulfate (50 g, 0.3 mol) was added dropwise with stirring to a solution of 2-cyanopyridine (25 g, 0.25 mol) in toluene (70 cm^3). After addition, the reaction mixture was heated for a further 4 h, then cooled to room temperature. The product formed as a dense pale yellow liquid, which was separated, washed with toluene and then hexane, dried under reduced pressure and finally *in vacuo* to yield a pale yellow solid (82% yield), mp 34–36 °C (Found: C, 46.47; H, 5.59; N, 9.79. [C$_8$H$_9$N$_2$][C$_2$H$_5$SO$_4$] requires C, 46.50; H, 5.46; N, 10.85%); δ_H (500 MHz, DMSO-*d*$_6$) 9.429 (1H, d, C(6)–H, J = 6.0 Hz), 8.81 (2H, m, C(3)–H and C(5)–H), 8.461 (1H, dd, J = 7 Hz), 4.834 (2H, q, J = 7.3 Hz), 3.719 (2H, q, J = 7.1 Hz), 1.620 (3H, t, J = 7.3 Hz), 1.086 (3H, t, J = 7.12 Hz); δ_H (500 MHz, MeCN-*d*$_3$) 9.27 (1H, d), 8.75 (1H, t), 8.59 (1H, d), 8.40 (1H, dd), 4.91 (2H, q), 3.90 (2H, q), 1.72 (3H, t), 1.21 (3H, t).

1-Ethyl-2-cyanopyridinium bis{(trifluoromethyl)sulfonyl}imide (32)

32 was prepared from **31** (21.8 g, 0.086 mol) in water (100 cm^3) and Li[NTf$_2$] (24.7 g) in water (100 cm^3). The product separated as a dense colourless liquid, which was washed with water and dried *in vacuo* to yield a colourless crystalline solid (85% yield), mp 36–38 °C (Found: C, 29.00; H, 2.19; N, 10.17. [C$_8$H$_9$N$_2$][NS$_2$O$_4$C$_2$F$_6$] requires C, 29.06; H, 2.19; N, 10.17%);

δ_H (500 MHz, MeCN-d_3) 9.429 (1H, d, C(6)–H, J = 6.0 Hz), 8.81 (2H, m, C(3)–H and C(5)–H), 8.461 (1H, dd, J = 7 Hz), 4.834 (2H, q, J = 7.3 Hz), 1.086 (3H, t, J = 7.12 Hz); δ_C (125.7 MHz, MeCN-d_3) 147.73, 146.49, 134.45, 131.97, 123.39, 120.84, 118.30, 117.11, 115.75, 109.96, 57.88, 14.52, 0.04.

1-Ethyl-2-cyanopyridinium hexafluorophosphate (33)

33 was prepared by the anion metathesis of **31** (4.5 g) in water (7.5 cm^3) with a solution of sodium hexafluorophosphate (3.5 g) in water (7.5 cm^3), resulting in a colourless powdery precipitate that was collected by filtration, dried in air and then *in vacuo*, mp 166–166 °C (Found: C, 34.39; H, 2.92; N, 10.02. [$C_8H_9N_2$][PF_6] requires C, 34.55; H, 3.36; N, 10.07%); δ_H (500 MHz, DMSO-d_6) 9.42 (1H, d, J = 5.9 Hz), 8.86 (1H, m), 8.83 (1H, m), 8.48 (1H, m), 4.85 (2H, q, J = 7.4 Hz), 1.644 (3H, t, J = 7.4 Hz).

1-Ethyl-4-(trifluoromethyl)pyridinium ethylsulfate (34)

4-(Trifluoromethyl)pyridine (1.91 g, 0.013 mol) and diethylsulfate (2.0 g, 1 equiv.) were dissolved in toluene (15 cm^3) and heated at 90 °C for 12 h with stirring in a sealed glass tube. The product formed initially as a cloudy suspension, which, when stirring and heating were stopped, settled as a dense lower phase. The upper toluene layer was removed, and the lower ionic liquid phase washed with toluene (10 cm^3) and hexane (10 cm^3). The remaining volatile solvents were then removed under reduced pressure and the ionic liquid was dried *in vacuo* as a colourless liquid (2.2 g), T_g = −84 °C; δ_H (500 MHz, D_2O) 1.165 (3H, t, J = 7 Hz), 1.566 (3H, t, J = 7 Hz), 3.960 (2H, q, J = 7 Hz), 4.680 (2H, q, J = 7 Hz), 8.3347 (2H, d, J = 6 Hz), 9.086 (2H, d, J = 6 Hz); δ_C (125.7 MHz, D_2O) 14.6, 15.9, 58.7, 66.0, 121.1 (CF_3, J = 274 Hz), 125.6 (C(3/5)), 145.2 (C(4)–CF_3, J = 37 Hz), 146.5 (C(2/6)); ESI-MS (MeCN/H_2O 1 : 1) +ve mode: 176.0682 ([cation]$^+$ calc, 176.0687); −ve mode 124.9901 ([$EtSO_4$]$^-$, 124.9909).

1-Ethyl-4-(trifluoromethyl)pyridinium bis{(trifluoromethyl)sulfonyl}imide (35)

The metathesis of **34** (2.1 g, 0.0073 mol) in water (10 cm^3) with Li[NTf_2] (2.1 g, 1 equiv.) in water (15 cm^3) resulted in separation of the ionic liquid as a dense colourless liquid, which was collected and washed with water (2 × 20 cm^3), and then dried *in vacuo* at 50 °C to give a colourless liquid that crystallised as blocky colourless crystals upon standing at room temperature, mp 28–29 °C; δ_H (500 MHz, DMSO-d_6) 1.58 (3H, t, J = 7.3 Hz, CH_3–CH_2N), 4.74 (2H, q, J = 7.3 Hz, CH_2–N), 8.68 (2H, d, J =6 Hz, C(3/5)–H), 9.45 (2H, d, J =6 Hz, C(2/6)–H); δ_C (125.7 MHz, DMSO-d_6) 16.6, 57.7, 119.9 (J = 319 Hz, CF_3–SO_2), 121.8 (J = 274 Hz, CF_3–C), 125.2 (C(3/5)), 143.2 (J = 35 Hz, C(4)–CF_3), 147.3 (C(2/6)); ESI-MS (MeCN/H_2O 1 : 1) +ve mode: 176.0685 ([cation]$^+$ calc, 176.0687), 632.0597 ([Q_2X]$^+$ calc 632.0547); −ve mode: 279.9029 ([anion]$^-$, 279.9173), 735.8893 ([QX_2]$^-$, 735.9033).

1-Ethyl-3-(trifluoromethyl)pyridinium ethylsulfate (36)

3-(Trifluoromethyl)pyridine (2.1 g, 0.014 mol) and diethylsulfate (2.2 g, 1 equiv.) were dissolved in toluene (15 cm^3) and heated at 90 °C for 12 h with stirring in a sealed glass tube. The product formed initially as a cloudy suspension, which, when stirring and heating were stopped, settled as a dense lower phase. The upper toluene layer was removed, and the lower ionic liquid phase was washed with toluene (10 cm^3) and hexane (10 cm^3). The remaining volatile solvents were then removed under reduced pressure and the ionic liquid was dried *in vacuo* as a colourless liquid (2.72 g), T_g = −99 °C; δ_H (500 MHz, D_2O) 1.18 (3H, t, J = 7 Hz), 1.57 (3H, t, J = 7 Hz), 3.98 (2H, q, J = 7 Hz), 4.66 (2H, q, J = 7 Hz), 8.20 (1H, dd, = J_1 = 6 Hz, J_2 = 8 Hz, C(5)–H), 8.80 (1H, d, J = 8 Hz, C(4)–H), 9.06 (2H, d, J = 6 Hz, C(6)–H), 9.37 (s, 1H, C(2)–H); δ_C (125.7 MHz, D_2O) 14.6, 15.9, 58.7, 66.0, 121.6 (CF_3, J = 270 Hz), 129.5 (C(5)), 131.2 (C(6)–CF_3, J = 37 Hz), 143.0 (C(2)), 143.2 C(4)), 147.9 (C(6)). ESI-MS (MeCN/H_2O 1 : 1); +ve mode: 176.0674 ([cation]$^+$ calc, 176.0687); −ve mode 124.9904 ([$EtSO_4$]$^-$, 124.9909).

1-Ethyl-3-(trifluoromethyl)pyridinium bis{(trifluoromethyl)sulfonyl}imide (37)

The metathesis of **36** (2.72 g, 0.009 mol) in water (15 cm^3) with Li[NTf_2] (2.56 g, 1 equiv.) in water (15 cm^3) resulted in separation of the ionic liquid as a dense colourless liquid, which was collected and washed with water (2 × 20 cm^3), and then dried *in vacuo* at 50 °C to give a colourless liquid, which solidified as a colourless crystalline mass after inducing nucleation by brief immersion in liquid nitrogen, mp 29–30 °C; δ_H (500 MHz, DMSO-d_6) 1.60 (3H, t, J = 7.3 Hz, CH_3–CH_2N), 4.73 (2H, q, J = 7.3 Hz CH_2–N), 8.42 (1H, dd, J_1 = 8.3 Hz J_2 = 6.3 Hz, C(5)–H), 9.07 (1H, d, J = 6.3 Hz, C(4)–H), 9.40 (2H, d, J = 8.3 Hz, C(6)–H), 9.76 (s, 1H, C(2)–H); δ_C (125.7 MHz, DMSO-d_6) 16.4, 57.7, 119.8 (J 324 Hz, CF_3–SO_2), 122.0 (J 274 Hz, CF_3–C), 129.3 (C(5)), 129.4 (C(6)–CF_3, J 36 Hz), 142.8 (C(2)), 143.7 C(4)), 148.7 (C(6)); ESI-MS (MeCN/H_2O 1 : 1) +ve mode: 176.0673 ([cation]$^+$ calc, 176.0687); −ve mode 279.9173 ([anion]$^-$, 279.9173), 735.9023 ([QX_2]$^-$, 735.9033).

Analysis

^{1}H NMR spectra were recorded on a Bruker Avance DRX 500 spectrometer in DMSO-d_6, D_2O, $CDCl_3$ or ethanenitrile-d_3. Melting points and glass transition temperatures were determined by differential scanning calorimetry (DSC) (Perkin-Elmer Pyris 1 DSC, equipped with cryostat cooling, 5–20 mg samples, 5 °C min^{-1} heating and cooling rates under nitrogen). Transitions above ambient temperature were confirmed optically by hot-stage polarising optical microscopy (Olympus BX50 microscope, equipped with a Linkam TH600 hot stage and TP92 temperature controller). Thermal decomposition profiles were collected by thermogravimetric analysis (TGA) (Perkin-Elmer Pyris 1 TGA with a 5 °C min^{-1} heating rate under nitrogen). IR data were recorded for twelve of the ionic liquid salts† (in the liquid state, between KBr disks, on a Perkin-Elmer Spectrum 100 FT-IR). Densities were determined at 10 °C intervals between 20 and 90 °C using an Anton Paar DMA4500 oscillating tube densitometer; the sample size was 1 cm^3. Measurements of kinematic viscosity were carried out over the temperature range 20 to 95 °C using a Brookfield DV-II+ cone and plate viscometer equipped with a Grant LTD6G circulating heater. The viscometer was fitted with luer-lock fittings, and a positive current of dry nitrogen was maintained at all times to ensure a dry sample environment and avoid the absorption of atmospheric moisture. Samples were introduced into the viscometer *via* a syringe and allowed to equilibrate for 15 min before data collection. Data was collected at intervals of 5 °C between 20–95 °C, or from the sample melting point to 95 °C for samples with higher melting points. The viscometer has a 1% accuracy and a 0.2% reproducibility; estimated uncertainty is better than 0.5 cPs. SAXS data were collected on a Philips XPERT-PRO diffractometer equipped with an Anton-Parr XRK-900 heating stage, using Cu-K$_\alpha$ radiation over the angle range 2θ = 2–50° at 25 and 95 °C.

X-ray crystallography

Samples of [C$_1$^{4}CNpy][MeSO$_4$] (**1**), [C$_1$^{4}CNpy][NTf$_2$] (**2**), [C$_2$^{4}CNpy][NTf$_2$] (**4**), [C$_1$^{3}CNpy][NTf$_2$] (**22**), [C$_2$^{3}CNpy][NTf$_2$] (**24**), [C$_2$^{2}CNpy][NTf$_2$] (**32**) and [C$_2$^{3}CF$_3$py][NTf$_2$] (**37**) were recrystallised by slow cooling of their melts. Crystals suitable for X-ray characterisation were grown from the supercooled dense ionic liquid phase, and crystal fragments were collected from the solid mass, mounted on fibres and transferred to the goniometer. Data for **1**, **2**, **32** and **37** were collected at the Advanced Light Source station 11.3.1 using a Bruker Platinum 200 CCD diffractometer with silicon ⟨111⟩ monochromated synchrotron radiation (λ = 0.77490 Å) at −80 °C, cooling with a stream of nitrogen gas. Bruker APEX2 and SAINT v7.3.4a[21] software was used for data collection and reduction. Data for **24** and **32** were collected on a Bruker-AXS SMART CCD diffractometer with graphite-monochromated Mo-K$_\alpha$ radiation (λ = 0.71073 Å) at room temperature using SAINT-N[22] software. Empirical absorption corrections were applied using SADABS,[23] and the structures were solved using direct methods and refined with SHELXTL v5.[24] Each structure was refined by full-matrix least-squares on F^2.

In each structure, the atoms were readily located by direct methods and all relevant connectivity established; the positions of all non-atoms in **1**, **4**, **22**, **24**, **32** and **37** were refined anisotropically, with the exception of **4** and **37**. Anion disorder was found in the structure of **4**, in which the central {–SO$_2$–N–SO$_2$–} portion of the anion was disordered over two sites, and the two –CF$_3$ groups also showed rotational disorder; both were modelled with an occupancy of 60 : 40. In the structure of **37**, a rotationally disordered –CF$_3$ group in the cation was refined isotropically over two positions with an occupancy of 50 : 50. Restraints used to model the disorder in both structures were added using the SAME instruction in SHELXTL to generate geometrically equivalent distances for the two occupancies.

For all the structures, hydrogen atoms were added at idealised positions. Crystals of **2** gave only poor quality diffraction data, which resulted in the higher *R*-value for the refinement; disorder of the anion –CF$_3$ groups is apparent, but was not explicitly modelled due to the poorer data quality.

Results and discussion

Synthesis

Functionalised 1-alkylpyridinium salts (Table 1) were prepared by alkylation of the corresponding cyano- and trifluoromethylpyridines with dimethylsulfate, diethylsulfate or bromoalkanes (butyl, hexyl, octyl, dodecyl or hexadecyl), followed by anion metathesis.

Table 1 Experimental characterisation of the ionic liquids prepared. Glass transition temperatures and melting points were determined by DSC and decomposition temperatures by dynamic TGA under nitrogen

	R	EWG	Anion	T_g/°C	mp/°C	T_{dec}/°C[a]
1	CH$_3$	4-CN	[MeSO$_4$]$^-$	—	108–115	244
2			[NTf$_2$]$^-$	—	65–66	294
3	C$_2$H$_5$		[EtOSO$_3$]$^-$	−71	—	230
4			[NTf$_2$]$^-$	—	33–35	355
5			[PF$_6$]$^-$	—	176	223/336
6	C$_4$H$_9$		Br$^-$	—	212	222
7			[NTf$_2$]$^-$	−64	—	350
8			[PF$_6$]$^-$	—	140	221/339
9	C$_6$H$_{13}$		Br$^-$	—	195–197	203
10			[NTf$_2$]$^-$	−59	10	310
11			[PF$_6$]$^-$	—	115	228/319
12	C$_8$H$_{17}$		Br$^-$	—	162	192
13			[NTf$_2$]$^-$	—	30	316
14			[PF$_6$]$^-$	—	122–124	214/335
15	C$_{12}$H$_{25}$		Br$^-$	—	196[b]	211
16			[NTf$_2$]$^-$	—	52	314
17			[PF$_6$]$^-$	—	146[c]	237/361
18	C$_{16}$H$_{33}$		Br$^-$	—	196[d]	255/350
19			[NTf$_2$]$^-$	—	68	309
20			[PF$_6$]$^-$	—	180[e]	200/320
21	CH$_3$	3-CN	[MeSO$_4$]$^-$	−68	—	232
22			[NTf$_2$]$^-$	—	63–65	299
23	C$_2$H$_5$		[EtOSO$_3$]$^-$	−71	—	243
24			[NTf$_2$]$^-$	—	73	322
25			[PF$_6$]$^-$	—	164–167	260
26	C$_4$H$_9$		Br$^-$	—	155–157	181
27			[NTf$_2$]$^-$	—[f]	—	320
28			[PF$_6$]$^-$	—	110–111	255
29	CH$_3$	2-CN	[MeSO$_4$]$^-$	—	91	258
30			[NTf$_2$]$^-$	—	19	251
31	C$_2$H$_5$		[EtOSO$_3$]$^-$	—	34–36	204
32			[NTf$_2$]$^-$	—	36–38	268
33			[PF$_6$]$^-$	—	164–166	264/383
34	C$_2$H$_5$	4-CF$_3$	[EtOSO$_3$]$^-$	−84	—	274
35			[NTf$_2$]$^-$	—	29–30	318
36		3-CF$_3$	[EtOSO$_3$]$^-$	−99	—	—
37			[NTf$_2$]$^-$	—	28–29	318

[a] Determined from the onset point to 5 wt% decomposition. [b] Solid–solid (83 °C). [c] Solid–solid (67 °C). [d] Solid–solid (85 °C), *lit*[18] solid–solid (61 °C), solid–S$_A$ (191 °C), S$_A$–*iso* (196 °C). [e] Solid–solid (75 and 86 °C). [f] No crystallisation or glass transitions were observed on cooling to −100 °C.

Twelve 1-alkyl-*n*-cyanopyridinium cations were prepared with differing alkyl substituents and nitrile-group positions. From 4-cyanopyridine, 1-alkyl-4-cyanopyridinium salts with methyl (**1** and **2**), ethyl (**3–5**), butyl (**6–8**), hexyl (**9–11**), octyl (**12–14**), dodecyl (**15–17**) and hexadecyl (**18–20**) substituents were prepared. For the two low symmetry (C_1) pyridines (3-cyanopyridine and 2-cyanopyridine), only cations with the shorter alkyl chain substituents were synthesised; 1-alkyl-3-cyanopyridinium with methyl (**21** and **22**), ethyl (**23–25**) and butyl (**26–28**) substituents, and 1-alkyl-2-cyanopyridinium with methyl (**29** and **30**) and ethyl (**31–33**) substituents were prepared to compare the effects of nitrile group substitution position across the three isomers.

Table 2 Comparison of the melting points of 1-ethyl-*n*-R-pyridinium bis{(trifluoromethyl)sulfonyl}imide salts (where R is the ring substituent, $-CH_3$, –CN or $-CF_3$) determined by DSC

Ionic liquid	Ring substituent	mp/°C
$[C_2{}^2pic][NTf_2]$[a]	2-CH_3	8
$[C_2{}^3pic][NTf_2]$[b]	3-CH_3	−5
$[C_2{}^4pic][NTf_2]$[c]	4-CH_3	12
$[C_2{}^2CNpy][NTf_2]$ (**32**)	2-CN	36–38
$[C_2{}^3CNpy][NTf_2]$ (**24**)	3-CN	73
$[C_2{}^4CNpy][NTf_2]$ (**4**)	4-CN	33–35
$[C_2{}^3CF_3py][NTf_2]$ (**36**)	3-CF_3	28–29
$[C_2{}^4CF_3py][NTf_2]$ (**35**)	4-CF_3	29–30

[a] 1-Ethyl-2-methylpyridinium. [b] 1-Ethyl-3-methylpyridinium. [c] 1-Ethyl-4-methylpyridinium.

The three 1-methyl-*n*-cyanopyridinium methylsulfate (**1**, **21** and **29**) and 1-ethyl-*n*-cyanopyridinium ethylsulfate (**3**, **23** and **31**) salts were prepared by alkylation of the corresponding cyanopyridine with dimethylsulfate or diethylsulfate, respectively, in toluene at 100 °C. In contrast to the highly exothermic reaction of dimethylsulfate and diethylsulfate with pyridine or 1-alkylimidazoles,[25] they reacted very slowly with cyanopyridines at room temperature to give turbid solutions after 12 h, consistent with the reduced basicity of EWG-functionalised pyridines. Increasing the temperature to 100 °C resulted in a smooth, controlled alkylation over *ca.* 6–8 h.

Similarly, heating the respective cyanopyridines with bromobutane under reflux, either neat or as a solution in toluene, yielded only traces of the alkylated products. Cyanopyridinum salts with butyl or longer substituents were synthesised as bromide salts by the alkylation of either 3-cyanopyridine or 4-cyanopyridine with the corresponding bromoalkane, in toluene at 135–160 °C in a sealed reactor under autothermal pressure. 4-Cyano- and 3-cyanopyridinium bromide salts were obtained in good yields as colourless (**6**, **9** and **26**) or yellow (**12**, **15** and **18**) precipitates on cooling of the yellow-orange reaction mixtures. 1-Butyl-2-cyanopyridinium bromide could not be prepared from bromobutane and 2-cyanopyridine under these conditions.

Anion metathesis with $Li[NTf_2]$ or $Na[PF_6]$ yielded the corresponding $[NTf_2]^-$ or $[PF_6]^-$ based hydrophobic 1-alkyl-*n*-cyanopyridinium salts. $[NTf_2]^-$ salts were isolated as either colourless ionic liquids (**7**, **10**, **13**, **27** and **30**) or colourless crystalline low melting point (mp < 75 °C) solids (**2**, **4**, **16**, **19**, **22**, **24** and **32**), and were dried *in vacuo*. **13** was initially isolated as a liquid, which then crystallised upon standing at room temperature over a period of weeks. The corresponding $[PF_6]^-$ salts (**5**, **8**, **11**, **14**, **17**, **20**, **25**, **28** and **33**) were all isolated as colourless precipitates, collected by filtration and dried in air.

The 1-ethyl-*n*-(trifluoromethyl)pyridinium ethylsulfate salts (**34** and **36**, n = 3 or 4) were synthesised as colourless oils in a similar manner from the corresponding *n*-(trifluoromethyl)-pyridine and diethylsulfate in toluene. Metathesis in water with $Li[NTf_2]$ gave the corresponding 1-ethyl-*n*-(trifluoromethyl)pyridinium bis{(trifluoromethyl)sulfonyl}imide salts (**35** and **37**) as hydrophobic liquids, which crystallised as low melting point solids upon drying. IR data were recorded for eleven of the ionic liquid salts, (**3**, **4**, **7**, **10**, **13**, **21**, **23**, **24**, **30**, **31** and **32**) in the liquid state.† The nitrile vibration was observed at around 2249.5 cm^{-1} with highly variable intensity, but with almost no variation in position (range 2246–2255 cm^{-1}), irrespective of the *N*-alkyl substituent or position of the nitrile group on the cation.

Phase transitions for all the salts were characterised by DSC and TGA, and are detailed in Table 1. Viscosity and density data were collected between the melting point of each salt and 100 °C for the examples that melted below 100 °C, and are shown in Table 2 and Table 3.

Table 3 Viscosity (/cP) for the ionic liquids **3**, **4**, **7**, **13**, **23**, **27**, **31**, **32**, **35** and **37** as a function of temperature in their respective liquid regions, within the temperature range 20–95 °C

T/°C	**3**	**4**	**7**	**13**[a]	**23**	**24**	**27**	**31**[a]	**32**[a]	**35**	**37**
20	8619				9946			1760			
25	4633		371	581	5839		1031	1075	610		
30	2615				3256			701		84	137
35	1440		186	301	1999		507	472	282		
40	954				1313			341		51	77
45	621		100	160	877		281	249	158		
50	457				604			183		34	49
55	330	92	65	94	433		186	133	94		
60	243				321			102		23	33
65	176	59	45	60	236		118	82	59		
70	135				185			67		16	22
75	102	40	32	47	133	43	75	56	40		
80	82				107			49		13	17
85	63	27	24	33	87	31	48	43	27		
90	52				72			38		10	13
95	45	20	18	25	58	21	32	34	23		
$\ln(A'/cP)$[b]	−5.16168	−7.0787	−3.98788	−3.96992	−5.66642		−10.3501	−3.59388	−4.92042	−4.8308	−4.81458
B'/K[b]	953.553	1554.22	606.221	681.518	1161.56		3138.11	612.615	790.342	721.898	745.656
T_0/K[b]	209.283	149.621	211.074	207.394	196.705		80.0928	218.953	201.582	190.541	194.709
R^2	0.99977	0.99980	0.99978	0.99941	0.99992		0.99921	0.99949	0.99948	0.99954	0.99975

[a] Lower temperature data collected from the super-cooled, metastable liquid. [b] Parameters from fitting the viscosity data to the VFT equation ($\eta = A'e^{(B'/T - T_0)}$), where R^2 is the goodness of fit.

Melting and glass transition temperature

All the salts with bromide and hexafluorophosphate anions were solids with melting points above 100 °C (see Table 1). In contrast, all the salts with flexible alkylsulfate and $[NTf_2]^-$ anions were liquids below 100 °C, with nine examples of room temperature ionic liquids (**3**, **7**, **10**, **21**, **23**, **27**, **30**, **34** and **36**). The presence of these anions leads to a reduction in the melting point of over 100 °C, compared with the corresponding hexafluorophosphate salts.

Melting point data were collected by DSC from the second heating cycle, after performing an initial heating and cooling cycle to anneal the sample. The phase behaviour was confirmed by visual inspection using a polarising optical microscope coupled with a thermal stage. All of the salts showed reversible crystallisation and melting transitions in the DSC experiments within the temperature range 10–200 °C (shown in Table 1), except for **3**, **7**, **21**, **23**, **34**, and **36**, where crystallisation could not be observed and the ionic liquid salts displayed only a glass transition. On cooling, **10** gave a low temperature glass transition that underwent cold crystallisation during the heating cycle to form a stable solid with a melting point of 10 °C.

The relative changes in melting points with alkyl chain length for the 1-alkyl-4-cyanopyridinium series with bromide, hexafluorophosphate and $[NTf_2]^-$ anions (**2–20**) are shown in Fig. 2. The variation in melting point with alkyl substituent appears to follow the same general trend found with other ionic liquids,[26] although interestingly, the position of maximum destabilisation of the solid state (lowest melting point) appears to vary with the anion (from octyl with bromide to hexyl with hexafluorophosphate); only a glass transition was obtained for **7** (butyl chain and $[NTf_2]^-$) further supporting these differences.

Solid–solid transitions were observed by DSC for the long chain 1-dodecyl-4-cyanopyridinium and 1-hexadecyl-4-cyanopyridinium bromide salts (**15** and **18**), and also the corresponding hexafluorophosphate analogues (**17** and **20**), consistent with the crystal–crystal transition reported previously for **18**.[18] The corresponding $[NTf_2]^-$ salts (**16** and **19**) did not show any polymorphism. Small angle powder X-ray scattering data were collected on four samples at 25 and 95 °C. A layered structure was observed, with expansion of the layer spacings at the higher temperature, and a change in the diffraction pattern consistent with the phase changes observed by DSC. In addition, the higher temperature diffraction data for the two hexafluorophosphate salts (**17** and **20**) showed collapse of the wide-angle diffraction peaks and the formation of a broad band around 4 Å, consistent with a transition to a plastic crystal phase with melted or disordered alkyl chains.[27] In earlier studies,[28] a similar solid–solid polymorphic transition was observed in liquid crystalline 1-alkyl-3-methylimidazolium salts, and was identified by a combination of small angle and single crystal X-ray diffraction to be a result of conformational reorganisation of the cationic head groups within the bulk bilayer structure of the crystals. It seems likely that a similar rearrangement occurs for **15**, **17**, **18** and **20**.

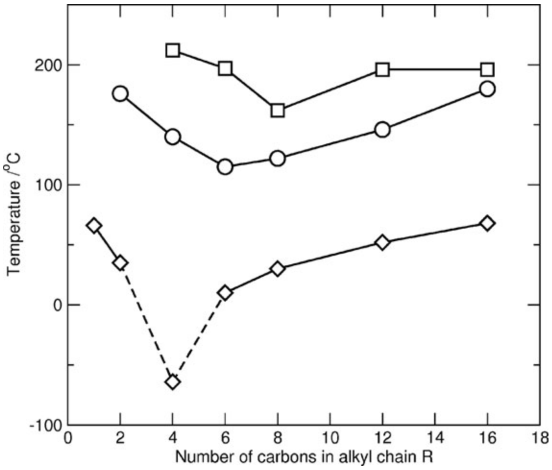

Fig. 2 Variation in the melting points of 1-alkyl-4-cyanopyridinium bromide (□), hexafluorophosphate (○) and $[NTf_2]^-$ (◇) salts with changing length of the alkyl substituent. Connecting lines are added as a visual aid, with a dashed line linking to the glass transition temperature of **7**.

Ionic liquids were obtained for 3-CN- and 2-CN-substituted 1-methyl-*n*-cyanopyridinium methylsulfate salts (**21** and **29**, respectively), whereas the 4-CN isomer formed a moderately high melting point crystalline solid (**1**, mp 108–115 °C). There is no clear pattern to the melting point variation with substitution position; **2** and **22** both melt around 65 °C, whereas the 2-cyano isomer, **30**, could not be crystallised.

Similarly, the three 1-ethyl-*n*-cyanopyridinium ethylsulfate salts (**3**, **23** and **31**) were all initially obtained as room temperature ionic liquids. Upon standing for one week, a sealed sample of **31** solidified as a colourless hygroscopic solid, whereas the other two isomers remained as liquids and gave only a low temperature glass transition during DSC.

In contrast, exchanging the anion for $[NTf_2]^-$ resulted in 2-cyano- and 4-cyano-substituted isomers (**4** and **32**) which had similar melting points that were *lower* by *ca.* 30 °C than that of the 3-cyano isomer, **24**. **34** and **36** formed room temperature ionic liquids, and the corresponding $[NTf_2]^-$ salts (**35** and **37**) were both isolated as crystals with identical low melting points (mp 28–30 °C) upon slow cooling of the molten ionic liquids.

The three 1-ethyl-*n*-cyanopyridinium hexafluorophosphate salts (**5**, **25** and **33**) have high melting points (164–176 °C), whereas the corresponding ethylsulfate (**3**, **23** and **31**) and 1-ethyl-*n*-(trifluoromethyl)pyridinium ethylsulfate (**34** and **36**) salts were glass-forming liquids, except for **31**, which crystallised as a low melting point solid (mp 34–36 °C). Similarly, four of the corresponding $[NTf_2]^-$ salts with either nitrile or trifluoromethyl functional groups (**4**, **25**, **32** and **37**) melt between 28–38 °C, with **24** melting at a higher temperature (73 °C).

The presence of the EWG increases the melting points of the salts compared with the corresponding pyridinium and *n*-methylpyridinium salts,[29,30] although no clear systematic trends with position of the functional group were observed.

For example, compared with the corresponding 1-butylpyridinium and 1-butyl-*n*-methylpyridinium bromide salts, the presence of the nitrile groups in **6** and **26** result in a stabilisation of the solid state by between 50–100 °C compared with the pyridinium salt (1-butylpyridinium bromide: mp 105 °C) and between 20–70 °C compared with the *n*-methylpyridinium salts (1-butyl-3-methylpyridinium bromide: mp 138 °C, 1-butyl-4-methylpyridinium bromide: mp 138 °C). Hexafluorophosphate salts **8** and **28** display melting points 65–95 °C higher than the corresponding 1-butyl-3-methylpyridinium hexafluorophosphate (46 °C) and 1-butyl-4-methylpyridinium hexafluorophosphate (44 °C) salts, but only 35–65 °C higher than 1-butylpyridinium hexafluorophosphate (75 °C).

Similarly, a comparison of the 1-ethyl-substituted $[NTf_2]^-$ salts **4**, **24**, **32**, **35** and **37** in Table 2 shows that the nitrile or trifluoromethyl substituents result in an increase in melting point by between ~20–80 °C.

This reversal of ordering between pyridinium and *n*-methylpyridinium salts demonstrates the difficulty of predicting trends in melting points and highlights the importance of specific crystal packing effects on the melting transition.

Thermal stability

The decomposition temperatures of the salts were investigated by dynamic TGA, scanning at 5 °C min^{-1} under nitrogen. It must be noted that this approach provides data on the thermal decomposition temperature and the relative stability of the materials, rather than on the absolute long term stability at any given temperature.[31] The results, shown in Table 1, are determined from the onset to 5% mass loss. All of the salts showed reasonable thermal stability. T_{dec} depends principally on the nature of anion present, with little variation between cations and, as anticipated, the salts with $[NTf_2]^-$ showed the greatest stability ($T_{dec} \approx$ 290–350 °C, except for the alkyl-2-cyanopyridinium salts). This was followed by the salts with hexafluorophosphate anions ($T_{dec} \approx$ 220–300 °C), with the initially synthesised alkylsulfate and bromide salts being significantly less stable ($T_{dec} \approx$ 180–250 °C).

It is notable that the methyl- and ethylsulfate salts (**1**, **3**, **21**, **23**, **29** and **31**) all decomposed, leaving a substantial volume of carbonaceous residue as a solid foam in the sample pans. The salts with hexafluorophosphate anions (**5**, **8**, **11**, **14**, **17** and **20**) all showed decomposition with an approximately 50% initial mass loss between 200–500 °C, followed by complete mass loss as part of a second thermal event between 320–350 °C. This behaviour is different to that observed previously for 1,3-dialkylimidazolium and 1-alkylpyridinium or 1-alkyl-*n*-methylpyridinium hexafluorophosphate salts,[32] where a single high temperature mass loss event characterises the decomposition.

Viscosity

Viscosity measurements were made between room temperature or the melting point and 95 °C for **3**, **4**, **7**, **13**, **23**, **27**, **31**, **21**, **35** and **37** using a cone and plate viscometer. In all cases, the viscosity decreased with temperature and showed a good fit to the VFT equation[33] characteristic of ionic liquids.[34] The corresponding data are summarised in Table 3 as a function of temperature.

Ionic liquids with the smallest cations and $[NTf_2]^-$ anions have the lowest relative viscosities. It is notable that at any given temperature, the trifluoromethyl-substituted ionic liquids (**35** and **37**) have the lowest viscosities of the ionic liquids studied.

The effect of the substitution position is not clear; for the isomeric 1-ethyl-*n*-cyanopyridinium ethylsulfate salts, the 2-cyano isomer (**31**) has the lowest viscosity at a given temperature, with the 4-cyano and 3-cyano isomers (**3** and **23**, respectively) having viscosities that are approximately equal to and double that of **31**. In contrast, the viscosities of the corresponding 1-ethyl-*n*-cyanopyridinium $[NTf_2]^-$ ionic liquids (**4**, **24** and **32**) were comparable over their common liquid regions.

Density

Table 4 shows the density measured for the liquid salts; these range between 1.25–1.56 g cm^{-3} and decrease linearly with increasing temperature.

The ionic liquids with $[NTf_2]^-$ anions have higher densities than the corresponding alkylsulfate salts (for example, comparing **3** and **4**). The density of the ionic liquids also decreases with increasing *N*-alkyl chain length. This corresponds to the introduction of low density methylene units (**4**, **7** and **13**) into the salts.

For each set of isomers, the 2-cyanopyridinium salts have the highest, and the 3-cyanopyridinum salts have the lowest, density in the liquid state, suggesting reduced cation–anion interactions in the liquid state and a larger effective cation volume for the 3-cyanopyridinium salts.

In contrast, in the crystal structures described below, isomerisation did not result in any significant changes in their solid state densities. For example, the standard deviation of

Table 4 Densities (/g cm^{-3}) of ionic liquids **3**, **4**, **7**, **13**, **23**, **27**, **31** and **32** as a function of temperature

T/°C	3	4[a]	7	13[a]	23	27	31[a]	32[a]
20	1.296	1.567	1.474	1.348	1.284	1.478	1.302	1.559
30	1.288	1.558	1.465	1.339	1.277	1.469	1.295	1.550
40	1.281	1.548	1.455	1.330	1.270	1.460	1.288	1.540
50	1.275	1.539	1.446	1.322	1.264	1.449	1.281	1.531
60	1.268	1.529	1.437	1.312	1.257	1.439	1.274	1.521
70	1.261	1.520	1.427	1.304	1.251	1.430	1.267	1.512
80	1.255	1.511	1.419	1.295	1.244	1.421	1.260	1.503
90	1.248	1.501	1.411	1.287	1.238	1.413	1.253	1.493
α^b	−6.762	−9.942	−9.095	−9.750	−6.560	−9.464	−7.000	−9.417
r^2	0.9992	0.9998	0.9991	0.9996	0.9996	0.9987	1.000	0.9998

[a] Data at 20 and 30 °C were collected from the supercooled liquids. [b] Coefficient of thermal expansion (/$\times 10^4$ K^{-1}), where r^2 is goodness of fit to the linear regression over the temperature range 20–90 °C.

Table 5 Crystal and refinement data

	1	2	4	22	24	32	37
Chemical formula	$[C_7H_7N_2]$ $[CH_3O_4S]$	$[C_7H_7N_2]$ $[C_2F_6NO_4S_2]$	$[C_8H_9N_2]$ $[C_2F_6NO_4S_2]$	$[C_7H_7N_2]$ $[C_2F_6NO_4S_2]$	$[C_8H_9N_2]$ $[C_2F_6NO_4S_2]$	$[C_8H_9N_2]$ $[C_2F_6NO_4S_2]$	$[C_8H_9F_3N]$ $[C_2F_6NO_4S_2]$
Formula weight	230.25	399.32	413.34	399.32	413.34	413.34	457.31
Crystal system	Orthorhombic	Monoclinic	Monoclinic	Monoclinic	Monoclinic	Orthorhombic	Triclinic
Space group	*Pna*2₁ (no. 33)	*P*21/*n* (no. 14)	*Cc* (no. 9)	*P*21/*n* (no. 14)	*P*21/*n* (no. 14)	*P*212121 (no. 19)	*P*-1 (no. 2)
a/Å	19.4965(15)	11.4431(11)	9.7224(12)	7.4620(6)	8.226(8)	12.290(16)	10.8446(15)
b/Å	8.5428(7)	11.8766(11)	10.7874(14)	26.715(2)	15.886(15)	13.84(2)	12.866(2)
c/Å	6.2274(5)	12.1955(11)	16.190(2)	7.8762(7)	12.553(12)	19.51(3)	13.2369(19)
α/°	90	90	90	90	90	90	90.366(5)
β/°	90	114.779(2)	103.573(2)	113.876(2)	91.871(18)	90	90.689(4)
γ/°	90	90	90	90	90	90	114.836(3)
V/Å^3	1037.20(14)	1504.8(2)	1650.6(4)	1435.7(2)	1640(3)	3318(8)	1675.8(4)
Z	4	4	4	4	4	8	2
D_c/g cm^{-3}	1.474	1.763	1.663	1.847	1.674	1.655	1.741
μ/mm^{-1}	0.436	0.617	0.568	0.646	0.410	0.406	0.590
F(000)	480	800	832	800	832	1664	879
T/K	193	193	193	193	298	298	193
$\theta_{\min,\max}$ (°)	2.3, 33.6	2.2, 33.7	2.8, 33.7	1.7, 33.6	2.1, 25.0	1.8, 25.0	1.7, 31.2
Reflections measured	24308	9483	11460	15064	15495	31744	19285
Independent reflections	3147	2032	4950	4287	2873	5837	8319
R_{int}	0.065	0.071	0.064	0.033	0.064	0.121	0.066
Observed data [$I > 2\sigma(I)$]	3079	1916	4268	3934	1738	2862	6004
No. parameters	137	219	215	217	227	452	487
Flack	0.05(7)	—	−0.04(17)	—	—	0.08(19)	—
R	0.0352	0.0990	0.1118	0.0449	0.0909	0.0775	0.0792
wR_2	0.1177[a]	0.3582[b]	0.3166[c]	0.1504[d]	0.2954[e]	0.2581[f]	0.2397[g]
GoF	1.15	1.78	1.27	1.15	1.04	1.01	0.99

[a] $w = 1/[\sigma^2(F_o^2) + (0.0827P)^2 + 0.0583P]$ where $P = (F_o^2 + 2F_c^2)/3$. [b] $w = 1/[\sigma^2(F_o^2) + (0.2000P)^2]$ where $P = (F_o^2 + 2F_c^2)/3$. [c] $w = 1/[\sigma^2(F_o^2) + (0.2000P)^2]$ where $P = (F_o^2 + 2F_c^2)/3$. [d] $w = 1/[\sigma^2(F_o^2) + (0.0879P)^2 + 0.4492P]$ where $P = (F_o^2 + 2F_c^2)/3$. [e] $w = 1/[\sigma^2(F_o^2) + (0.1327P)^2 + 4.5618P]$ where $P = (F_o^2 + 2F_c^2)/3$. [f] $w = 1/[\sigma^2(F_o^2) + (0.1022P)^2 + 4.3509P]$ where $P = (F_o^2 + 2F_c^2)/3$. [g] $w = 1/[\sigma^2(F_o^2) + (0.1286P)^2 + 2.5580P]$ where $P = (F_o^2 + 2F_c^2)/3$.

the densities of the three 1-ethyl-*n*-cyanopyridinium $[NTf_2]^-$ isomers is less than 1%. The one exception is **22**, where a major change in the $[NTf_2]^-$ anion conformation from the lower energy *trans* form to the less common, higher energy *cis* form[35,36] enables more efficient packing of the ions and formation of a higher density crystal.

X-Ray crystallography

Crystalline samples suitable for single crystal X-ray diffraction were obtained for **1**, and for six $[NTf_2]^-$ salts with 1-methyl- or ethyl-substituted pyridinium cations containing nitrile (**2**, **4**, **22**, **24** and **32**) or trifluoromethyl (**37**) functions on the ring. In all cases, crystals or crystal fragments suitable for single crystal X-ray analysis were obtained by slow cooling of the neat ionic liquid to room temperature. The structures were solved by direct methods. Crystal data and refinement details are shown in Table 5.† Powder XRD data on bulk samples was consistent with the single crystal data, confirming the composition of the bulk material. The structures of **1**, **2**, **4**, **22** and **24** contained a single ion pair in the asymmetric unit, whereas the asymmetric units of **32** and **37** contained two ion pairs. Structural disorder was found and modelled in the anion of **4**, and in a trifluoromethyl group cation of **37**.

For consistency, in the discussion of the structures below, the hydrogen atoms of the pyridinium cation ring are denoted by their substitution positions, rather than by crystallographic labels, *i.e.* C(2)–H is the hydrogen *ortho* to the nitrogen, *etc.*

In the structure of **1**, the 1-methyl-4-cyanopyridinium cation is planar and forms close contact hydrogen-bonding interactions with two methylsulfate anions in the plane of the cation ring, with short contacts from C(2)–H to two oxygen atoms of one anion at 2.42 and 2.52 Å; the anion also accepts a hydrogen bond from the N–CH_3 group of the cation at 2.53 Å. The corresponding C(6) position of the cation provides a hydrogen bond donating site to two oxygen atoms of a second anion, with hydrogen–oxygen distances of 2.39 and 2.42 Å (Fig. 3).

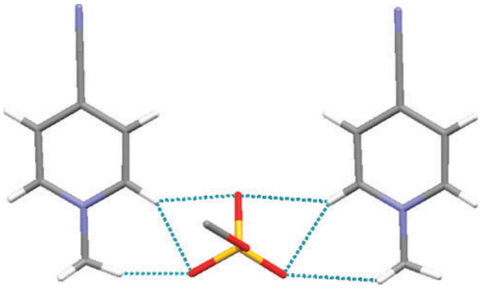

Fig. 3 Hydrogen-bonding from cation C(2/6)–H and N–CH_3 positions to the anion in **1**; the hydrogen atoms of the methylsulfate anion are removed for clarity.

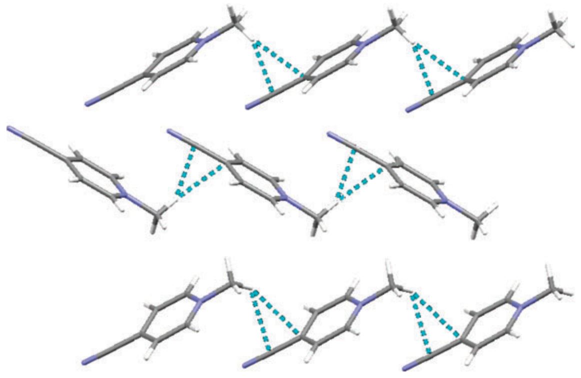

Fig. 4 Cation–cation packing in the crystal structure of **1**, showing the formation of the alternating herringbone packing of cations.

The most striking feature of the crystal packing in **1** is the formation of a herringbone pattern of cations (Fig. 4), in which cations are oriented head-to-tail in each layer, so that the N–CH_3 group of one cation overlays a nitrile group of the adjacent cation, with a cation–cation separation of 3.35 Å. This stacking also leads to the formation of alternating layers containing exclusively nitrile or N–CH_3 groups.

The close packing of the ions in **2**, containing the $[NTf_2]^-$ anion, shows a much clearer influence of the cation nitrile group as a hydrogen bond acceptor compared to structure **1** with a methylsulfate anion. The $[NTf_2]^-$ anion adopts the low energy all-*trans* configuration, with a $F_3C\cdots CF_3$ dihedral angle of 175.8°. Short contacts between cations and anions are observed between three of the cation ring hydrogens and the oxygen atoms of neighbouring anions (in the range 2.32–2.46 Å, shown in Fig. 5).

In contrast to the overlapping stacks of cations observed for **1**, hydrogen bonds from each C(2)–H of the cation to two nitrile groups of adjacent cations in **2** (C(2)–H$\cdots$N$\equiv$C, 2.68 and 2.72 Å) produce a four cation cluster, with two donors and two nitrile acceptors (Fig. 6). This motif propagates through the crystal to form double-layered sheets of cations separated by anions.

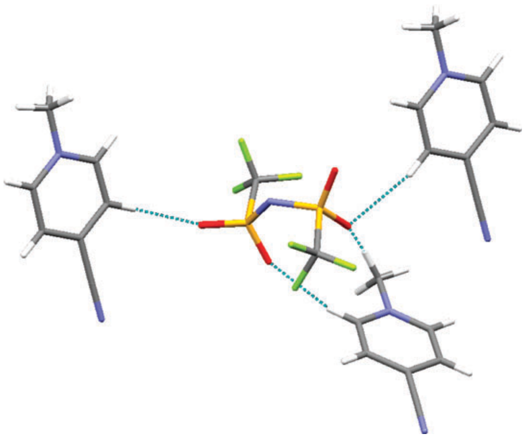

Fig. 5 Hydrogen-bonding from cation C(2/6)–H and N–CH_3 positions to the anion in **2**.

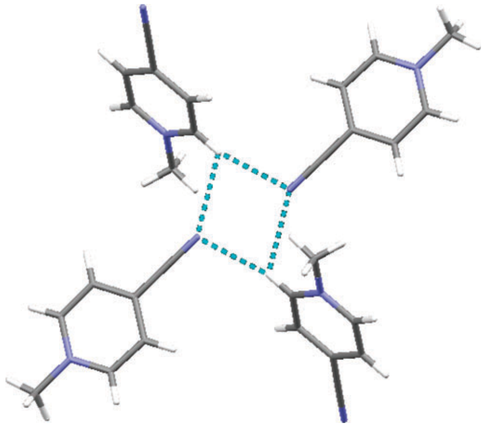

Fig. 6 Cation–cation packing in the crystal structure of **2** forming a four cation cluster.

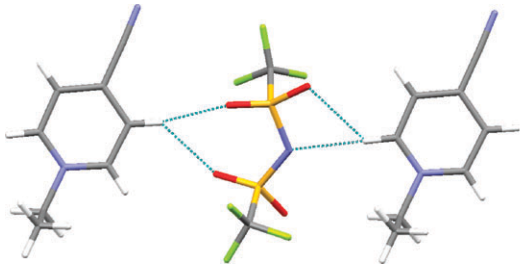

Fig. 7 Alternating cation–anion hydrogen-bonding in the plane of the cation ring formed through bifurcated C(3)–H$\cdots$O and C(6)–H$\cdots$O/N hydrogen bonds to the major anion conformation in **4** (only the major occupancy of the disordered anion is shown for clarity).

The structure of **4** shows changes to accommodate the more bulky 1-ethyl-4-cyanopyridinium cation, in which the ethyl group is twisted perpendicular to the plane of the pyridinium ring. The central –SO_2–N–SO_2– portion of the anion was found to be disordered in the structure and was modelled over two sites with an occupancy of 40 : 60, with common positions for the –CF_3 moieties. Both anion conformations have an all-*trans* conformation, with a $F_3C\cdots CF_3$ dihedral angle of 171.8°. In-plane packing of the cations and anions occurs through bifurcated hydrogen bonds from the C(3)–H and C(6)–H positions of the cation to the anion oxygen and nitrogen atoms (Fig. 7), with the N-atom interaction alternating between C(3)–H and C(6)–H in the two disordered anion positions. The closest cation–cation interaction occurs with the nitrile group acting as a hydrogen bond acceptor from an N–CH_2-hydrogen (2.50 Å), and also from a pyridinium ring C(2)–H hydrogen at a slightly longer distance of 2.85 Å (Fig. 8), forming head-to-tail chains of cations.

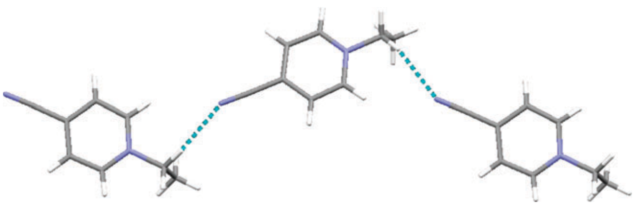

Fig. 8 The cation–cation packing and closest contacts in the crystal structure of **4** produce cation chains.

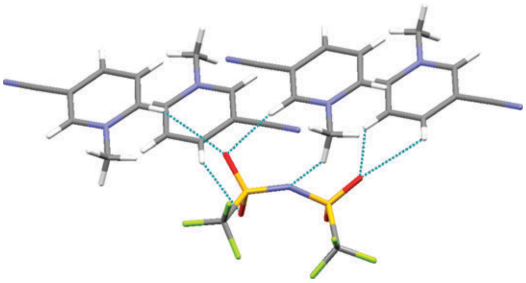

Fig. 9 Cation–anion hydrogen-bonding in the structure of **22**.

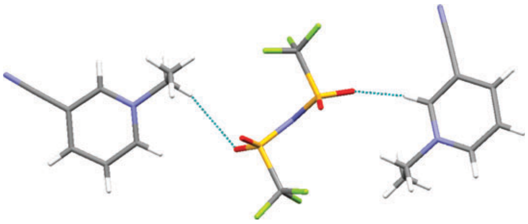

Fig. 11 Cation–anion hydrogen-bonding in **24** from the C(2)–H and methylene C(7)–H positions of the cation to anion oxygens in the cation plane.

The effect of changing the nitrile group position on the cation can clearly be seen in the crystal structure of **22**, where the anion adopts the less common higher energy *cis*-conformation, with a $F_3C\cdots CF_3$ dihedral angle of 13.3°. This anion conformation, which has also been observed with 1,3-dimethylimidazolium and Group 1 metal $[NTf_2]^-$ salts,[36–38] leads to the formation of a layered structure containing fluorous sheets formed from the $–CF_3$ groups of anions separated by charged layers of cations and anion $SO_2–N–SO_2$ moieties. Short cation–anion hydrogen-bonding contacts are observed from the C(2)–H and C(6)–H hydrogens of the cations to the nitrogen (and oxygen) atoms of the anion at <2.5 Å, and from the $N–CH_3$ group, which penetrates into the anionic layer of the structure and leads to methyl–trifluoromethyl contacts (C–H···F–C = 2.53 Å) (Fig. 9).

The electron-withdrawing and inductive effects of the nitrile group lead to an increase in cation polarisation and a net positive charge on the C(5)–H position. This is manifested in the crystal structure as a strongly directing cation–cation hydrogen bond from the pyridinium ring C(5)–H position to a nitrile group (2.38 Å) of an adjacent cation in the plane of the structural layers (Fig. 10).

The polarisation of the cation also results in a strongly structuring hydrogen bond between C(5)–H and the nitrile groups of cations in the 1-ethyl-3-cyanopyridinium analogue, **24**. The increased bulk of the *N*-alkyl substituent on the cation precludes the formation of crystals that are isostructural with **22**. Instead, **24** forms a structure containing sheets of anions and cations, in which the anion adopts the more conventional all-*trans* conformation. The *N*-ethyl group of the cation is oriented perpendicular to the ring, with a torsion angle of 84.0°. Cation–anion interactions of the C(2)–H (ring) and $N–CH_2$ groups of the cation with the oxygen atoms of anions at 2.50 and 2.57 Å fix two anions, one either side of the cations at right angles to the hydrogen-bonded cation chains. This generates two-dimensional sheets (Fig. 11), which pack with overlaying anions and capping pyridinium rings in adjacent layers. On the face containing the ethyl substituent, the anion approaches the cation through the sulfonyl oxygen, which points directly at the centre of the ring (distance to centroid = 2.89 Å). On the opposite face, the central nitrogen atom of the anion is placed over the ring with a slightly larger separation (distance to centroid = 3.29 Å).

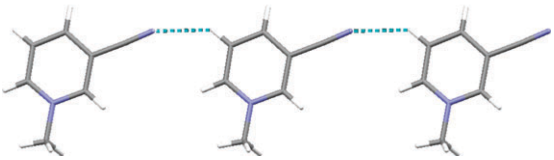

Fig. 10 Cation–cation packing, showing the directional $C(5)–H\cdots N{\equiv}C$ hydrogen bond in the crystal structure of **22**.

Cation–cation hydrogen bonds from C(5)–H and C(6)–H to the nitrile group of the nearest cation lead to the formation of linear arrays of cations with co-planar pyridinium rings (Fig. 12). Polarisation of the charge distribution in the 1-alkyl-3-cyanopyridinium cations leads to the formation of well-defined cation–cation hydrogen bonds, although the motif changes between **22** and **24** as a consequence of packing effects.

In **32**, similar conformations were found for the two cations and two anions in the asymmetric unit. The *N*-ethyl group of the cation is oriented almost perpendicular to the ring, with torsion angles of 79.0 and 84.3°. Both $[NTf_2]^-$ anions are found in the fully extended *trans*-configuration. Both anions are surrounded by five cation nearest neighbours, four of which form hydrogen bonds from aromatic ring hydrogens to oxygen atoms of the anion (Fig. 13). There are additional $CF_3\cdots F_3C$ (2.939 Å) contacts between adjacent anions of symmetry-inequivalent anions. In contrast to the structures of **1**, **2**, **4**, **22** and **24**, the cation–cation interactions in **32** are longer; the closest contacts (shown in Fig. 14) from aromatic ring hydrogen atoms to nitrile groups are 2.71 and 2.75 Å from C(3)–H and C(4)–H, and 2.79 Å from C(5)–H, respectively.

37, which contains a trifluoromethyl-substituted cation, also crystallised with two ion pairs in the asymmetric unit cell. Both cations have essentially identical conformations, with the ethyl substituent being oriented perpendicular to the plane of the pyridinium ring. In one cation, the trifluoromethyl substituent shows significant rotational disorder, indicated by the larger probability ellipsoids for the fluorine atoms. The anions adopt

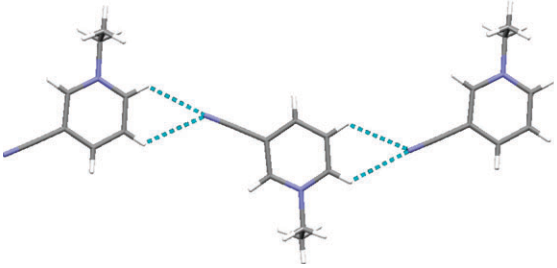

Fig. 12 Cation–cation packing, showing the two hydrogen bonds from C(5)–H and C(6)–H to the nitrile acceptor in the crystal structure of **24**.

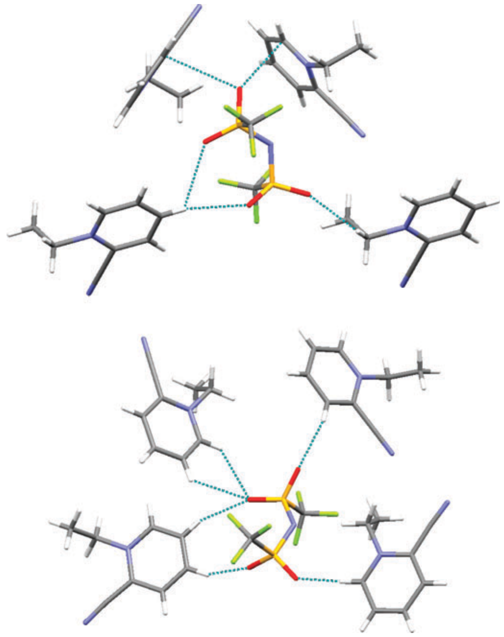

Fig. 13 Cation–anion hydrogen-bonding to the two anions in the asymmetric unit of **32**.

the low energy *trans*-conformation that is common for $[NTf_2]^-$, with $F_3C\cdots CF_3$ dihedral angles of 173.1 and 160.4°. Each cation is bounded by two anions that are positioned equatorially about the pyridinium ring. One anion accepts a bifurcated hydrogen bond from the pyridinium C(2)-position to two oxygen atoms, one on either side of the anion, and two to the same oxygen atom from the N–CH_2 group of the cation. The second equatorial anion accepts hydrogen bonds on one side only, from the N–CH_2 and C(6)–H groups of the cation (Fig. 15). In contrast to all the other structures obtained, there is no discernable cation–cation hydrogen-bonding in **37**; the closest contacts between cations occurs through the approach of $-CF_3$ and $-CH_3$ groups of adjacent cations (Fig. 16).

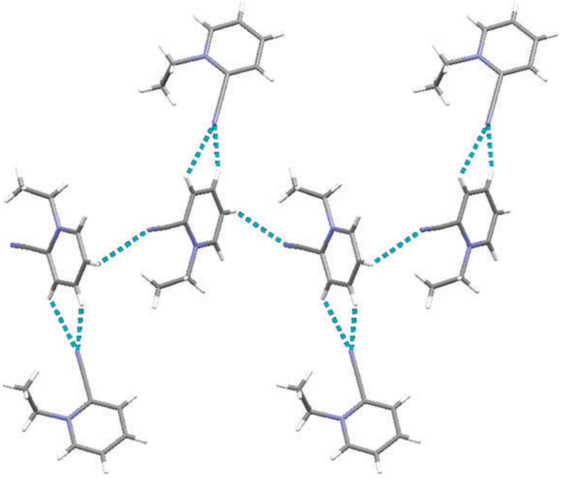

Fig. 14 Cation–cation closest contacts and packing in the crystal structure of **32**.

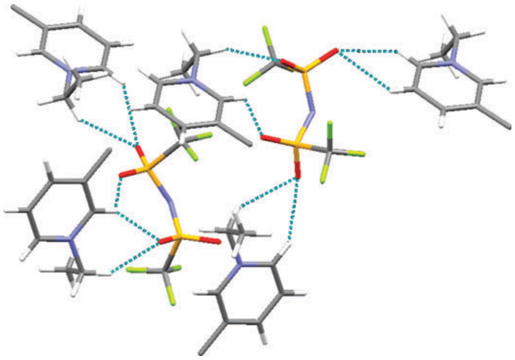

Fig. 15 Cation–anion hydrogen-bonding to the two independent anions in **37**. Fluorine atoms from the cation $-CF_3$ groups have been removed for clarity.

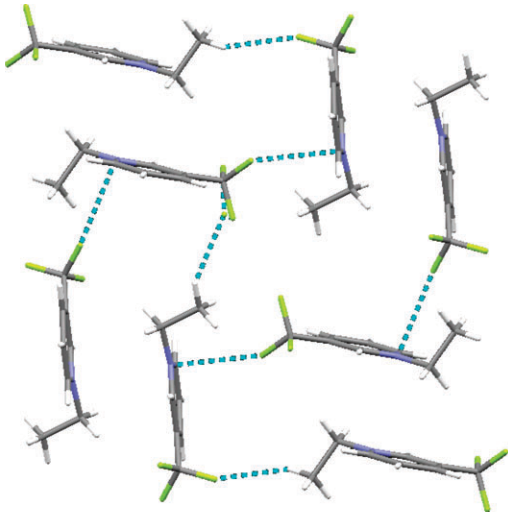

Fig. 16 Cation–cation closest contacts and packing in the crystal structure of **37** (only one position of the disordered $-CF_3$ group (C(7)F(1–3)) in the cation is shown for clarity).

Cation–cation hydrogen-bonding resulting from the polarisation of the charge distribution in the cation and induced by the presence of the EWG has a significant structuring effect in the crystal structures on the $[NTf_2]^-$ salts **2**, **4**, **22** and **24**, and has a much less pronounced effect on **32**, in which the nitrile group is in the 2-position. There are essentially no cation–cation interactions shorter than the van der Waals distance for the trifluoromethyl-substituted salt **37**. The only salt crystallographically characterised with a methylsulfate anion, **1**, displays a completely different packing motif, with staggered layers of co-planar cations separated by the van der Waals distance.

Conclusions

A series of pyridinium-based ionic liquids that incorporate nitrile or trifluoromethyl electron-withdrawing functions in the charge-carrying region of the ionic liquid cation have been prepared and characterised. In contrast to previously reported ionic liquids with nitrile functions appended to the cation alkyl chains, the electrostatic charge of the cation is significantly perturbed by derivatisation with electron-withdrawing groups and results in a stabilisation of the solid state relative to the unsubstituted analogues. This results in a corresponding reduction in the liquid range of the ionic liquids, although a number of examples with flexible anions (alkylsulfate or bis{(trifluoromethyl)sulfonyl}imide) anions were liquid from below room temperature. Significantly, all the nitrile- and trifluoromethyl-functionalised 1-ethylpyridinium bis{(trifluoromethyl)sulfonyl}-imide salts melted just above room temperature to give stable, relatively low viscosity ionic liquids.

The influence of cation derivatisation using EWGs on the electronic and liquid structure of these ionic liquids,[39] and on their solvent interactions with electron donor solutes is currently under active investigation. The results will be reported in due course.

Acknowledgements

The authors gratefully acknowledge BP, QUILL and the EPSRC (Portfolio Partnership Scheme, Grant EP/D029538/1) for funding. The Advanced Light Source is supported by the Director, Office of Science, Office of Basic Energy Sciences of the U.S. Department of Energy under contract no. DE-AC02-05CH11231. W. M. R would like to acknowledge the support of Paul Trulove and Hugh De Long. Portions of this work were funded by the U.S. Air Force Office of Scientific Research and the U.S. Naval Academy. Any opinions, findings, and conclusions or recommendations expressed in this material are those of the author(s) and do not necessarily reflect the views of the U.S. Air Force or Navy.

References

1 *Ionic Liquids in Synthesis*, ed. P. Wasserscheid and T. Welton, Wiley-VCH, Weinheim, 2nd edn, 2008.

2 A. R. Katritzky, A. Lomaka, R. Petrukhin, R. Jain, M. Karelson, A. E. Visser and R. D. Rogers, *J. Chem. Inf. Comput. Sci.*, 2002, **42**, 71; A. R. Katritzky, R. Jain, A. Lomaka, R. Petrukhin, M. Karelson, A. E. Visser and R. D. Rogers, *J. Chem. Inf. Comput. Sci.*, 2002, **42**, 225; D. M. Eike, J. F. Brennecke and E. J. Maginn, *Green Chem.*, 2003, **5**, 323; I. López-Martin, E. Burello, P. N. Davey, K. R. Seddon and G. Rothenberg, *ChemPhysChem*, 2007, **8**, 690.

3 A. R. Katritzky, H. Yang, D. Zhang, K. Kirichenko, M. Smiglak, J. D. Holbrey, W. M. Reichert and R. D. Rogers, *New J. Chem.*, 2006, **30**, 349.

4 A. R. Katritzky, S. Singh, K. Kirichenko, J. D. Holbrey, M. Smiglak, W. M. Reichert and R. D. Rogers, *Chem. Commun.*, 2005, 868; A. R. Katritzky, S. Singh, K. Kirichenko, M. Smiglak, J. D. Holbrey, W. M. Reichert, S. K. Spear and R. D. Rogers, *Chem.–Eur. J.*, 2006, **12**, 4630.

5 J. D. Holbrey, A. E. Visser, S. K. Spear, W. M. Reichert, R. P. Swatloski, G. A. Broker and R. D. Rogers, *Green Chem.*, 2003, **5**, 129.

6 G. W. Meindersma, A. J. G. Podt and A. B. de Haan, *Fuel Process. Technol.*, 2005, **87**, 59.

7 A. Arce, M. J. Earle, H. Rodríguez and K. R. Seddon, *Green Chem.*, 2007, **9**, 70.

8 J. D. Holbrey, W. M. Reichert, M. Nieuwenhuyzen, O. Sheppard, C. Hardacre and R. D. Rogers, *Chem. Commun.*, 2003, 476; M. Deetlefs, C. Hardacre, M. Niewenhuyzen, O. Sheppard and A. K. Soper, *J. Phys. Chem. B*, 2005, **109**, 1593.

9 J. D. Holbrey, I. López-Martin, G. Rothenberg, K. R. Seddon, G. Silvero and X. Zheng, *Green Chem.*, 2008, **10**, 87.

10 S. Tsuzuki, M. Mikami and S. Yamada, *J. Am. Chem. Soc.*, 2007, **129**, 8656.

11 D. Zhao, Z. Fei, R. Scopelliti and P. J. Dyson, *Inorg. Chem.*, 2004, **43**, 2197; D. Zhao, Z. Fei, T. J. Geldbach, R. Scopelliti and P. J. Dyson, *J. Am. Chem. Soc.*, 2004, **126**, 15876.

12 Z. Fei, D. B. Zhao, D. Pieraccini, W. H. Ang, T. J. Geldbach, R. Scopelliti, C. Chiappe and P. J. Dyson, *Organometallics*, 2007, **26**, 1588.

13 P. Bonhôte, A.-P. Dias, M. Armand, N. Papageorgiou, K. Kalyanasundaram and M. Grätzel, *Inorg. Chem.*, 1996, **35**, 1168.

14 T. L. Merrigan, E. D. Bates, S. C. Dorman and J. H. Davis Jr, *Chem. Commun.*, 2000, 2051.

15 M. Pal and S. Bagchi, *J. Chem.Soc., Faraday Trans. 1*, 1985, **81**, 961; D. A. Binder and M. M. Kreevoy, *J. Phys. Chem. A*, 1997, **101**, 1774.

16 J. W. Larsen, A. G. Edwards and P. Dobi, *J. Am. Chem. Soc.*, 1980, **102**, 6780.

17 S. V. Lymar, R. F. Khairutdinov, V. A. Soldatenkova and J. K. Hurst, *J. Phys. Chem. B*, 1998, **102**, 2811.

18 D. P. Jackson and B. M. Fung, *Mol. Cryst. Liq. Cryst.*, 1997, **303**, 73.

19 E. Takahashi, F. Sanda and T. Endo, *J. Appl. Polym. Sci.*, 2004, **91**, 3470.

20 R. A. Mackay and E. J. Poziomek, *J. Am. Chem. Soc.*, 1970, **92**, 2432.

21 *APEX2 v.1.0-22* and *SAINT v7.34a* User Manuals, Bruker AXS Inc., Madison WI 53719, 2004.

22 *SAINT-NT*,Bruker AXS Inc., Madison, WI, 1998.

23 G. M. Sheldrick, *SADABS, Program for area detector adsorption correction*, Institute for Inorganic Chemistry, University of Göttingen, Germany, 1996.

24 G. M. Sheldrick, *SHELXTL, version 50.5*, Siemens Analytical X-Ray Instruments Inc., Madison, WI, 1996.

25 J. D. Holbrey, W. M. Reichert, R. P. Swatloski, G. A. Broker, W. R. Pitner, K. R. Seddon and R. D. Rogers, *Green Chem.*, 2002, **4**, 407.

26 J. D. Holbrey and K. R. Seddon, *J. Chem. Soc., Dalton Trans.*, 1999, 2133.

27 W. A. Henderson and S. Passerini, *Chem. Mater.*, 2004, **16**, 2881; M. Forsyth, J. Huang and D. R. MacFarlane, *J. Mater. Chem.*, 2000, **10**, 2259.

28 A. E. Bradley, C. Hardacre, J. D. Holbrey, S. Johnston, S. E. J. McMath and M. Nieuwenhuyzen, *Chem. Mater.*, 2002, **14**, 629; A. Downard, M. J. Earle, C. Hardacre, S. E. J. McMath, M. Nieuwenhuyzen and S. J. Teat, *Chem. Mater.*, 2004, **16**, 43.

29 J. M. Crosthwaite, M. J. Muldoon, J. K. Dixon, J. L. Anderson and J. F. Brennecke, *J. Chem. Thermodyn.*, 2005, **37**, 559.

30 A. Noda, K. Hayamizu and M. Watanabe, *J. Phys. Chem. B*, 2001, **105**, 4603.

31 M. Kosmulski, J. Gustafsson and J. B. Rosenholm, *Thermochim. Acta*, 2004, **412**, 47; T. M. Wooster, K. M. Johanson, K. J. Fraser, D. R. MacFarlane and J. L. Scott, *Green Chem.*, 2006, **8**, 691.

32 C. M. Gordon, J. D. Holbrey, A. R. Kennedy and K. R. Seddon, *J. Mater. Chem.*, 1998, **8**, 2627.

33 G. Tammann and W. Hesse, *Z. Anorg. Allg. Chem.*, 1926, **156**, 245; G. S. Fulcher, *J. Am. Ceram. Soc.*, 1925, **8**, 339; H. Vogel, *Phys. Z.*, 1921, **22**, 645.

34 R. A. Carpio, L. A. King, R. E. Lindstrom, J. C. Nardi and C. L. Hussey, *J. Electrochem. Soc.*, 1979, **126**, 1644; A. A. Fannin Jr, D. A. Floreani, L. A. King, J. S. Landers, B. J. Piersma, D. S. Stech, R. L. Vaughn, J. S. Wilkes and J. L. Williams, *J. Phys. Chem.*, 1984, **88**, 2614.

35 M. Herstedt, M. Smirnov, P. Johansson, M. Chami, J. Grondin, L. Servant and J. C. Lassègues, *J. Raman Spectrosc.*, 2005, **36**, 762.

36 L. Xue, C. W. Padgett, D. D. DesMarteau and W. T. Pennington, *Solid State Sci.*, 2002, **4**, 1535.

37 J. D. Holbrey, W. M. Reichert and R. D. Rogers, *Dalton Trans.*, 2004, 2267.

38 Z. Zak, A. Ruzicka and C. Michot, *Z. Kristallogr.*, 1998, **213**, 217.

39 C. Hardacre, J. D. Holbrey, C. L. Mullan, M. Nieuwenhuyzen, T. G. A. Youngs and D. T. Bowron, *J. Phys. Chem. B*, 2008, **112**, 8049.